# DEVELOPMENT OF ADAPTIVE CONTROL TECHNIQUES FOR NUMERICALLY-CONTROLLED MILLING MACHINES

## INTERIM TECHNICAL DOCUMENTARY PROGRESS REPORT NR. IR II

1 January 1963 - 31 July 1963

Fabrication Branch

Air Force Materials Laboratory

Research and Technology Division

Air Force Systems Command

United States Air Force

Wright-Patterson Air Force Base, Ohio

ASD Project Nr. 7-713



**Phase II of a program directed toward the development of adaptive control techniques for numerically controlled milling machines is described, and plans for Phase III are reviewed. The detailed design of a complete adaptive control system was completed, and plans were made for fabrication and checkout of the system in Phase III. An experimental metalcutting program was conducted to develop techniques for on-line measurement of process performance. The instantaneous tool wear rate was found to correlate with certain of the sensed variables, and an empirical equation for calculation of this parameter was developed. Attempts to correlate surface microfinish with sensed variables have thus far been unsuccessful, and additional experimental work is required.**

(Prepared under Contract AF 33(657)-8782 by The Bendix Corporation, Research Laboratories Division, Southfield, Michigan)

## NOTICES

When U.S. Government drawings, specifications, or other data are used for any purpose other than a definitely related Government procurement operation, the Government thereby incurs no responsibility nor any obligation whatsoever; and the fact that the Government may have formulated, furnished, or in any way supplied the said drawings, specifications, or other data is not to be regarded by implication or otherwise, as in any manner licensing the holder or any other person or corporation or conveying any rights or permission to manufacture, use, or sell any patented invention that may in any way be related thereto.

Copies should not be returned to the Aeronautical Systems Division unless return is required by security considerations, contractual obligations, or notice on a specific document.

# FOREWORD

This Interim Technical Documentary Progress Report covers the work performed under AF 33(657)-8782 from 1 January 1963 to 31 July 1963 (Phase II). It is published for technical information only and does not necessarily represent the recommendations, conclusions, or approval of the Air Force.

This contract with the Bendix Corporation, Research Laboratories Division, is being accomplished under the technical direction of Mr. William Webster of the Advanced Fabrication Techniques Branch, Air Force Materials Laboratory, Research and Technology Division, Wright-Patterson Air Force Base, Ohio.

Mr. Ronald M. Centner of the Research Laboratories, Control and Data-Handling Systems Department, Information and Control Systems Laboratory, is the engineer in charge. Others who cooperated materially in the research and in the preparation of this report were Dr. E. C. Johnson, Manager of the Information and Control Systems Laboratory; Mr. K. V. Bailey, Head of the Control and Data-Handling Systems Department; Mr. P. Maker, Staff Engineer; Mr. D. C. Kowalski, Senior Engineer; Mr. J. M. Idelsohn, Engineer; Mr. R. A. Valek, Engineer; Mr. J. E. Miramonti, Senior Test Engineer. This report has been given the Research Laboratories Division internal number 2373.

The primary objective of the Air Force Manufacturing Methods Program is to develop, on a timely basis, manufacturing processes, techniques, and equipment for use in economical production of USAF materials and components. This program encompasses the following technical areas:

Rolled Sheet, Forgings, Extrusions, Castings, Fiber and Powder Metallurgy Component Fabrication, Joining, Forming, Materials Removal, Fuels, Lubricants, Ceramics, Graphites, Non-Metallic Structural Materials, Solid State Devices, Passive Devices, Thermionic Devices.

Your comments are solicited on the potential utilization of the information contained herein as applied to your present or future production programs. Suggestions concerning additional Manufacturing Methods development required on this or other subjects will be appreciated.

## PUBLICATION REVIEW

Approved by: K.V. Bailey

K.V. Bailey
Head - Control and Data-Handling Systems Department

Approved by: E.C. Johnson

E.C. Johnson
Head - Information and Control Systems Laboratory

ABSTRACT-SUMMARY
Interim Technical
Documentory Report

# DEVELOPMENT OF ADAPTIVE CONTROL TECHNIQUES FOR NUMERICALLY CONTROLLED MILLING MACHINES

R. M. Centner

The Bendix Corporation
Research Laboratories Division

Phase II of a program directed towards the development of adaptive control techniques for numerically controlled machine tools is described, and plans for Phase III are reviewed.

In Phase I of this project, literature searches and studies of the milling process and of optimizing computer techniques were completed. These efforts led to the development of a conceptual design for an adaptive controller. The major function of the adaptive controller is to automatically adjust feed and speed values so as to optimize the process performance with respect to preselected criteria on cost and/or production rate. A secondary function of the controller is to assure that system operation remains within a set of constraints and thereby produces parts of acceptable quality.

Early in Phase II a computer simulation study of the complete adaptive control system was performed. This study was completed successfully and served to validate the basic logic that had been conceived during Phase I.

Following successful completion of the simulation study, the detailed design of the adaptive controller was initiated. This effort was completed and fabrication of the controller will begin at the start of Phase III. The first model of the controller will contain approximately 95 printed circuit cards.

An experimental metalcutting program was conducted during Phase II. The purpose of this program was to develop techniques for on-line measurement of cutting performance factors. After some initial difficulties, a suitable instrumentation system was developed and a large body of data was accumulated, primarily for climb milling of 4140 steel. An empirical equation was developed for calculation of the instantaneous tool wear rate as a function of feed, speed, and sensed variables. Error analyses have indicated that this equation is sufficiently

accurate to be used in the first model of the adaptive control system. Attempts to correlate surface microfinish to sensed variables have been generally unsuccessful to date, although there is some indication that tool vibration signals may contain the necessary information. The experimental program also served to establish reasonable constraint values for a number of the important variables.

The planned activity for Phase III includes fabrication and checkout of the adaptive controller, interconnection of the controller to the numerical control system, and initial checkout of the total adaptive control system. It is also planned to continue the experimental metal-cutting program to further verify the results achieved to date, to develop an on-line microfinish measurement technique, and possibly to broaden the results to a wider range of materials and cutting processes.

TABLE OF CONTENTS

LIST OF ILLUSTRATIONS

# SECTION 1

# INTRODUCTION

The general objective of this project is the development of adaptive control techniques for application to numerically controlled milling machines. The advent of numerical control has materially improved the production rate and quality of milled aerospace components, by closing control loops around the moving members of the machine. In this case the use of position feedback enables accurate control of both the relative position and relative velocity of the workpiece and the cutting tool. Selection of the desired values of these quantities must be accomplished by the part programmer. The positional information is explicitly obtained from the geometric requirements of the finished part, and is normally a straightforward computational problem. However, the selection of velocity commands such as cutter speed and feedrate is largely empirical, based upon a combination of experience and handbook data. These velocity commands directly affect the production rate and machining cost, and have a significant effect on quality aspects such as surface finish and dimensional accuracy.

The use of empirical techniques to select speed/feed values cannot be expecte to yield optimum performance. The reasons for this fact include variations in workpiece metallurgy, variations in cutter sharpness, unpredictable chatter effects on surface finish, and variation between handbook data obtained under controlled laboratory environments and actual performance obtained in production environments. The use of analytical techniques to predict optimum or nearly optimum speed/feed values would be a formidable, if not impossible, task.

Adaptive control is a technique which offers the potential of on-line optimization of machine performance. To achieve adaptive control, sensors are used for on-line measurement of machining variables such as tool-tip temperature and spindle torque. The sensor outputs are applied to an adaptive controller, which calculates the overall system performance and then adjusts the feed and speed so as to improve the performance. This process continues until the performance approaches optimum. Thereafter, the controller adapts to changes in the characteristics of the tool and material by resetting the feed and speed so as to maintain optimum performance at all times.

The specific objectives of this project are to develop, test, and demonstrate an adaptive controller applied to a modern numerically controlled milling machine. The project is divided into four phases, as listed below.

Phase I - Investigation and study
Phase II - Development and validation of components and subsystems
Phase III - Assembly, test, and modification of the total system
Phase IV - Operation, evaluation, and demonstration of the total system

The Phase I final report, which corresponded to the First Interim Technical Documentary Progress Report, was published in December 1962.

This report contains a description of work accomplished during Phase II, which began on 1 January 1963 and concluded on 31 July 1963. Also included are a schedule and discussion of plans for Phase III, plus conclusions and recommendations regarding the status of the project and the potential for ultimate success.

## SECTION 2

## WORK ACCOMPLISHED DURING PHASE II

### 2.1 SUMMARY

In Phase II the design of the first model of the adaptive control system was essentially completed. The work accomplished was divided into two major areas: (1) design of the adaptive controller, and (2) performance of an experimental metal-cutting program.

At the completion of Phase I the conceptual design of the adaptive controller had been completed, and the basic logic for two alternative optimizing strategies had been developed. The first work accomplished in Phase II was a simulation study of the over-all adaptive control system. As a result of this study, a particular optimizing strategy was selected and the basic logic flow was finalized. The simulation study also served to confirm the validity of the system concept and the ability of the system to function in the presence of drift and noise.

Following completion of the simulation study, effort was devoted to the detailed design of the adaptive controller. The design utilized an existing family of printed circuit cards manufactured by the Bendix Industrial Controls Division. To meet the specific requirements of the adaptive controller, minor modifications to a few circuits were required. The necessary modifications were completed and verified by a small amount of subsystem testing.

The detailed design of the first model of the adaptive controller has now been completed. Wiring lists and circuit card assignments have been prepared, and all manual controls have been designed into the system. All major parts have been ordered, and many have been received. Fabrication of the controller will begin at the start of Phase III.

In addition to completing the design of the adaptive controller itself, effort was also given to the interface between the controller and the Bendix DynaPath numerical control system. The detailed design of the interface logic was completed, and necessary modifications to the DynaPath system have been specified.

The experimental metalcutting program began early in Phase II and continued for a period of five months. The major objectives of the program were: (1) the development of techniques for on-line measurement of tool wear rate, and (2) the establishment of suitable constraints to ensure production of acceptable parts. The first half of the program was devoted to development of a suitable instrumentation system, and the second half was devoted to the gathering of experimental data. The most difficult and time-consuming aspect of the instrumentation system was the development of a suitable spindle torque dynamometer. The two major problems encountered in this area were the occurrence of bending moments and the inability of the torque measuring system to withstand high peak cutting torques. The bending moment problem was solved by fabrication of a specially designed coupling between the spindle drive system and the dynamometer. However, this coupling was not able to withstand high torques, thereby limiting the depth of cut which could be used in the program. The experience gained during this effort has led to the design of a completely new dynamometer system which should be superior to the system used in Phase II. It is planned to fabricate and install this new system early in Phase III, and to use it for the remainder of the project.

Nearly all of the experimental data was gathered by peripheral milling of AISI 4140 steel, using a climb cut and a two-inch-diameter end mill cutter. Analysis of this data resulted in the development of an empirical equation for calculating the tool wear rate as a function of metal removal rate, tool-tip temperature, and spindle torque. Based on this expression, comparison of calculated wear rates with actual wear rate values has shown a reasonable correlation. Further analysis has indicated that, in the large majority of cases, errors inherent in the use of the empirical equation will have only a slight degrading effect on the ultimate performance of the system. To date, this conclusion can be applied only to the cutting of 4140 steel under the range of conditions used in the test program. However, there is a high degree of confidence that the general approach can be extrapolated to a wide range of workpiece materials and cutting conditions. Further experimental work is necessary to substantiate this belief.

The establishment of constraint limits to assure acceptable surface microfinish has proven to be difficult. No definite correlation was established between the microfinish and any of the sensed variables, although there is evidence that the frequency spectrum

of the tool vibration signal may contain the information. Additional experimentation using more detailed processing of the vibration signal is required. Until specific correlation data is obtained, it is planned to use a constraint limit on maximum amplitude of the vibration signal to prevent the occurrence of excessive chatter. Data was obtained during the experimental program to enable the selection of a number of other constraints and reasonable values for their limits.

## 2.2 ADAPTIVE CONTROLLER

During Phase II the design of the adaptive controller was completed and a simulation study was conducted to verify the system concept and the optimization logic. This section describes the system design and summarizes the simulation study. The over-all design concept and the physical characteristics of the system are described in Sections 2.2.1 and 2.2.2, respectively. Sections 2.2.3 through 2.2.6 describe in further detail the major subsystems and the interface with the numerical control system. The simulation study is summarized in Section 2.2.7.

### 2.2.1 Over-all System Design

The basic system concept that was presented in the Phase I final report has thus far proven to be valid. This concept is illustrated in Figure 2-1, which is a block diagram of a complete machine control system including both numerical position control and adaptive feed/speed control.

The programmed input data is sensed by a tape reader or similar entry device and entered into the numerical control system. This data includes dimensional coordinates, feed* and spindle speed. Consider first the operation of the system without adaptive control. The numerical control system converts the input data to servo command signals, and the servo drives position the machine axes so as to generate the desired contour at the programmed rate, with the spindle rotating at the programmed speed. Feedback transducers sense the actual motions and compare them with the command signals to assure accurate

*In this report the term "Feed" will denote inches of slide travel per spindle revolution and the term "Feedrate" will denote inches of slide travel per minute. Conversion from one form to the other is easily accomplished, since (feedrate) = (feed) x (spindle speed).

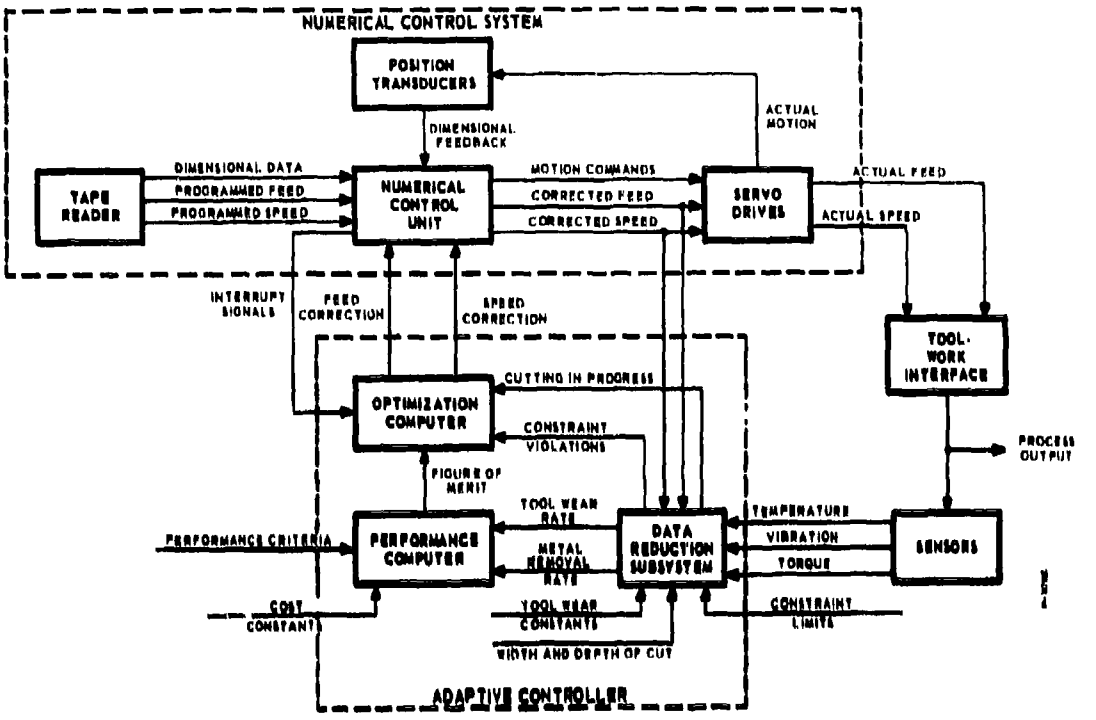


Figure 2-1 - System Block Diagram

execution of the commands. However, the actual process output, which is in reality the condition and shape of the finished part, is removed from the feedback points by the effects at the tool-work interface. Since these effects are complex and difficult to predict, the process output will not conform precisely to that desired by the programmer. To achieve good control of the finished part, it is often necessary to program the feed and speed conservatively low.

To add adaptive control to the system, additional feedback information is obtained from the process output by means of sensors coupled as closely as possible to the tool-work interface. The sensor signals, which represent the variables torque, vibration, and temperature, are applied to the adaptive controller. The controller contains three major parts: a data reduction subsystem, a performance computer, and an optimization computer.

The data reduction subsystem generates two analog output signals and a number of on/off signals known as "constraint violations." The analog outputs correspond to tool wear rate in inches per minute and metal removal rate in cubic inches per minute. The constraint violation signals indicate whether various aspects of the machine performance are within predetermined limits. The quantities constrained to maximum and/or minimum values include torque, speed, feed, horsepower, and vibration. The purpose of constraint detection is to assure that acceptable parts are produced and to minimize the possibility of damage to the machine and the tool. In addition to the sensor outputs, the data reduction subsystem receives feed and speed information from the numerical control system, plus a group of externally entered constants. The externally entered constants include the constraint limits, the width and depth of cut, and tool wear constants which depend upon the workpiece and tool materials and upon the type of cut. In the initial model of the adaptive controller, all constants will be entered as potentiometer settings. In future versions it will be possible to store some of the constants on the program tape.

The performance computer operates upon the tool wear rate and metal removal rate signals to generate a figure of merit for the system performance. The figure of merit is defined by the equation

$$H = \left| \frac{MRR}{K_1 + \frac{(K_1 \tau + K_2 B)}{W_o} (TWR_c)} \right|_{0 \leq B \leq 1}$$

where:

$H$ = figure of merit - $(in.^3/\$)$,

$MRR$ = metal removal rate - $(in.^3/min)$,

$TWR_c$ = calculated tool wear rate - $(in./min)$,

$K_1$ = direct labor rate + overhead rate - $(\$/min)$,

$K_2$ = cost per grind + initial tool cost/maximum number of regrinds - $(\$)$,

$\tau$ = downtime required to change tools - $(min)$,

$W_o$ = maximum allowable wear before regrinding - $(inches)$.

The quantity B, which is denoted as the base of the figure of merit, is used to set the performance criteria. If B is set equal to one, the criteria is machining cost and the units of H are cubic inches per dollar. If B is set equal to zero, the criteria is production rate and the figure of merit expression reduces to

$$H = \left[\frac{1}{K_1}\right] \left| \frac{MRR}{1 + \frac{\tau}{W_o} (TWR_c)} \right|$$

in which case H is a measure of cubic inches per minute. Intermediate values of B would result in a performance criteria which is a compromise between cost and production rate. The constants used in the calculation of H are all externally entered by means of potentiometers. The derivation of the figure of merit equation was given in the Phase I final report[1].

The optimization computer receives the figure of merit information from the performance computer and adjusts the feed and speed values in such a manner as to maximize the value of H. The computer operates on a sampled-data basis, i.e., the value of H is sampled periodically and a feed/speed adjustment is made after each sampling. The constraint violation signals are sent directly from the data reduction subsystem to the optimization computer. The occurrence of a violation at any time interrupts the normal optimization logic and initiates a special subroutine which operates to change the feed and speed so as to return to an acceptable performance condition. After the constraint violation has been removed, the system returns to normal operation. Certain other operational conditions, such as slewing and deceleration, may also require interruption or modification of the normal optimization cycle. These conditions are made known to the optimization computer by special interrupt signals from the numerical control unit and by a "cutting not in progress" signal from the data reduction subsystem. These special conditions are discussed further in Section 2.2.5.

### 2.2.2 Physical Characteristics of the System

The adaptive controller uses a combination of analog and digital computing techniques to perform its function. The data reduction subsystem and the performance computer use primarily analog techniques, and the optimization computer uses mainly digital techniques. The circuitry is entirely solid-state and is packaged on printed circuit cards

approximately 3.5 inches by 4.5 inches in size. It is estimated that the complete system will use a total of 95 cards plus one magnetostrictive delay line for data storage. It is planned to house the first model of the system in a standard relay rack about 47 inches high. This rack will include, in addition to the main circuitry, a system power supply and necessary lights, switches, etc. for operating the system.

A sketch of the planned external appearance of the system is shown in Figure 2-2. Potentiometers are used to set in most of the system constants, and binary coded toggle switches are used to select the initial feed and speed setpoints. Since this will be the first operating model of the adaptive controller, it was felt that the use of manual inputs would provide a useful flexibility and decrease the effort required to check out and evaluate the system. Future models of the system would, of course, use tape-programmed data for the feed and speed values and also for selecting some of the system constants.

The design of the adaptive controller utilized an existing family of printed circuit cards manufactured by the Bendix Industrial Controls Division. Consequently, more than 80% of the circuit cards to be used in the system are standard off-the-shelf items. The remaining cards are slightly modified versions of standard units. A small amount of breadboard testing was performed during Phase II to verify the circuit modifications and to check out some of the more critical subsystems. This testing was completed satisfactorily.

In general, the design concept of the adaptive controller could be applied to any milling machine which has closed-loop feedrate and spindle speed control. However, the detailed design is intimately related to the specific characteristics of the basic machine control system. The initial model of the adaptive controller was designed to work with a Bendix DynaPath numerical control system having the features of automatic feedrate control and automatic spindle speed control. Timing signals are provided to the adaptive controller by the DynaPath system, and the delay line storage elements in the two systems are synchronized. In principle, there should be no difficulty in applying the adaptive controller to other numerical control systems, but the extent of practical problems would depend upon the specific characteristics of the system.

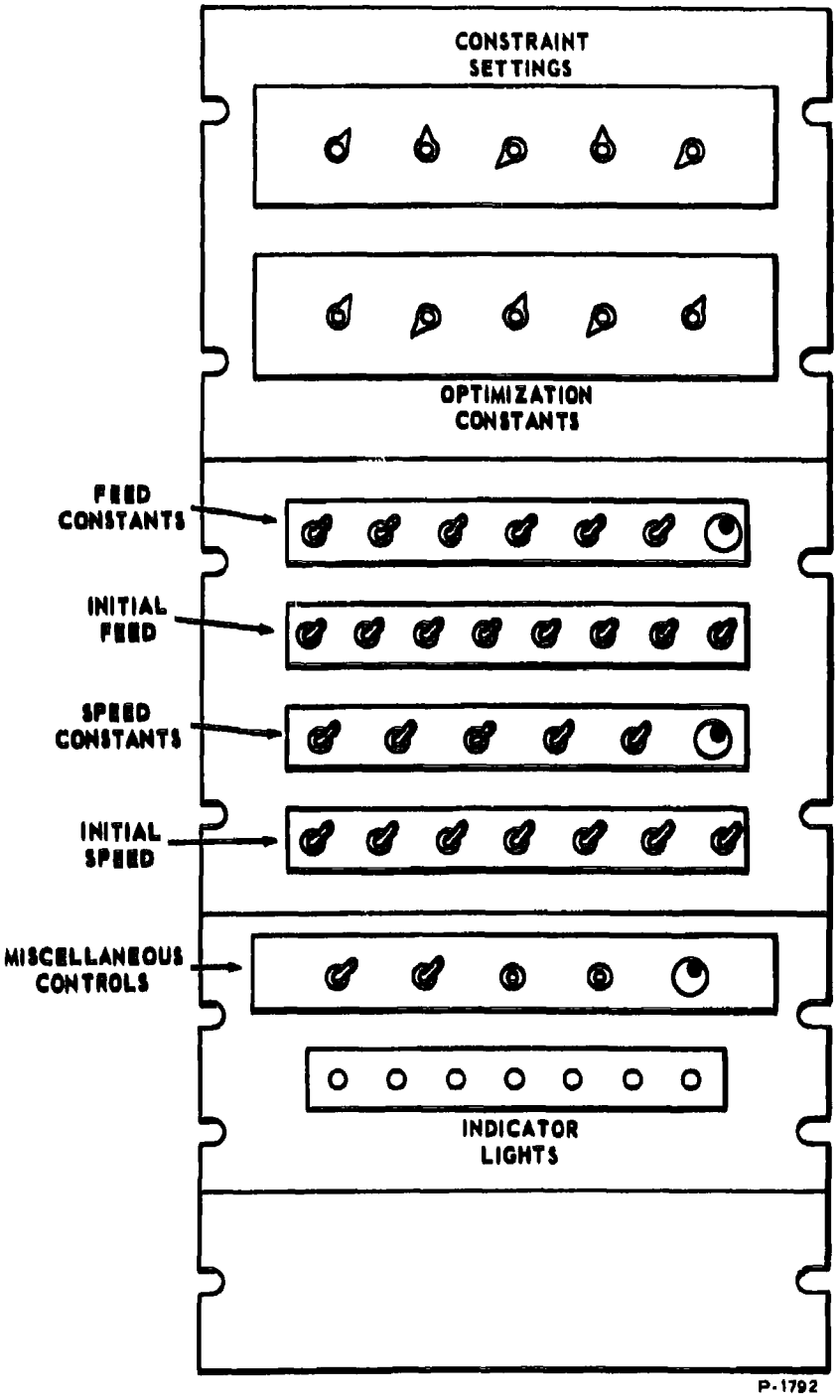


Figure 2-2 - Sketch of Adaptive Controller Control Panels

### 2.2.3 Data Reduction Subsystem

The function of this subsystem is to reduce data taken from various points of the system to data directly usable by the balance of the adaptive controller. The inputs are voltage analogs and potentiometer settings. The outputs are analog voltages proportional to metal removal rate and tool wear rate, binary coded signals indicating the occurrence of constraint violations, and a special control signal indicating whether cutting is in progress. Figure 2-3 is a block diagram of the data reduction subsystem. The various operations which take place within this subsystem are described in the following paragraphs. The electronics used to convert sensor outputs to the desired form and impedance levels are not discussed specifically in this section, but are covered in Appendix I.

#### 2.2.3.1 Metal Removal Rate

The metal removal rate is given by the equation

$$MRR = F_{wd}$$

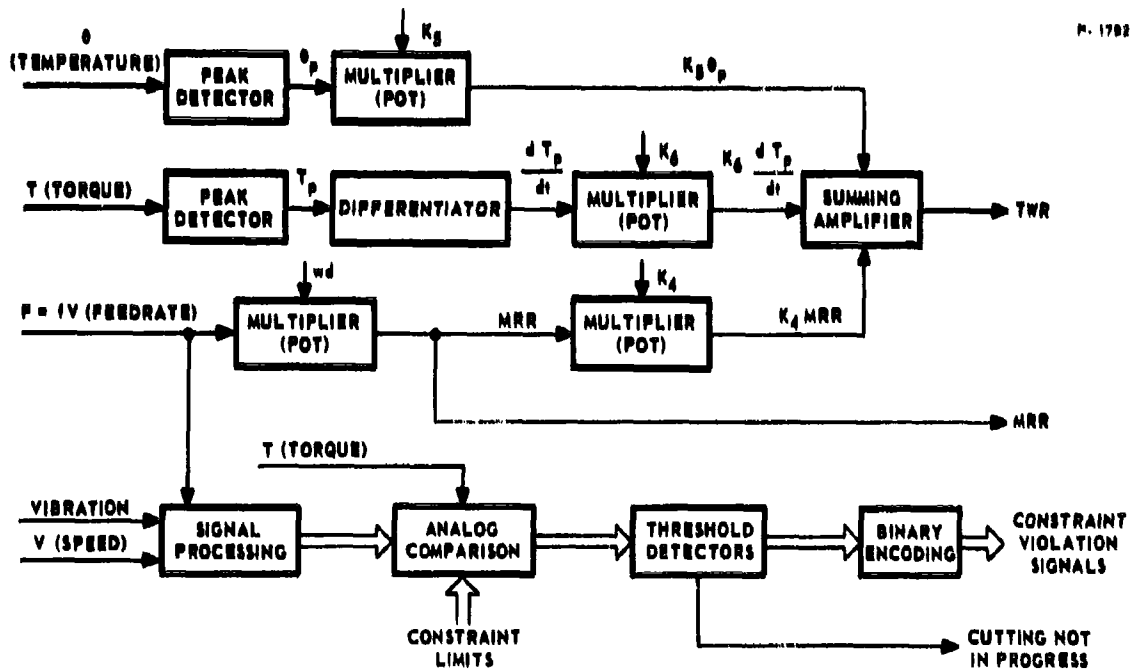


Figure 2-3 - Block Diagram of Data Reduction Subsystem

where: $F$ = feedrate - (in./min),

$w$ = width of cut - (in.),

$d$ = depth of cut - (in.).

The quantity wd is an operator-entered constant and the feedrate is given by

$$F = fV$$

where: $f$ = feed per revolution - (in./rev),

$V$ = spindle speed - (rev/min).

Thus

$$MRR = (fV)(wd)$$

A d-c voltage proportional to the value of fV is available from the automatic feedrate portion of the numerical control system. Thus, the MRR signal is produced as a negative analog voltage by straightforward multiplication, as shown in Figure 2-3.

#### 2.2.3.2 Tool Wear Rate

As a result of the experimental metalcutting program, an empirical equation has been developed for the computation of tool wear rate. This equation is

$$TWR_c = K_5 MRR + K_6 \theta_p + K_7 \frac{dT_p}{dt}$$

where: $TWR_c$ = calculated tool wear rate - ($in.^3$/min),

$K_5, K_6, K_7$ = weighting factors,

$\theta_p$ = peak value of amplified thermocouple voltage - (volts),

$\frac{dT_p}{dt}$ = the time derivative of peak spindle torque - (in.-lb/min).

The development of this equation and the accuracy with which it represents the true value of TWR is discussed in Section 2.3.3.

The weighting factors are related to the particular characteristics of the tool, workpiece and machine, and are entered into the system by setting calibrated potentiometers. In practice, the operator or programmer would select these values based upon nomographs or handbook data. The value of MRR is calculated as described in the preceding section. A tool-work thermocouple is used as a sensor to produce a voltage proportional to the average tool-tip temperature. The thermocouple output voltage is amplified and processed through a peak detector to obtain $\theta_p$. A strain-gage sensor is used to measure the spindle torque, T, by unbalancing a resistance bridge. The torque signal is used directly by the constraint violation detectors without further processing. For the TWR computation, a peak detector is used to obtain $T_p$ and then a differentiating circuit to obtain $dT_p/dt$. The three properly weighted quantities are combined in a summing amplifier to produce $TWR_c$. The computation is entirely analog, and the output is expressed as a negative d-c voltage.

#### 2.2.3.3 Constraint Violation Detection

Each of the constraint violation signals is binary coded as logic "1" for a violation condition and logic "0" for a no-violation condition. The following seven constraints are imposed upon the system:

(1) HP-actual < HP-max ; HP = spindle horsepower

(2) T-actual < T-max ; T = spindle torque

(3) V-actual < V-max ; V = spindle speed

(4) V-actual > V-min

(5) f-actual < f- max ; f = feed per revolution

(6) f-actual > f- min

(7) VIB-actual < VIB-max ;VIB = tool vibration

In addition to the seven constraints, the system also determines whether T-actual is greater than a preset minimum value, T-min. This signal is used to determine whether cutting is in progress by setting T-min approximately equal to the torque required to drive the spindle when no metal is being cut.

Figure 2-4 is a detailed block diagram of the constraint violation detectors. The input quantities include d-c voltage analogs of actual torque, T, spindle speed, V, and absolute feedrate, fV, plus an a-c signal proportional to tool vibration. The constraint limits and the T-min value are set in by calibrated potentiometers. Violation of constraints (2), (3), (4) and (7), plus the value of the "cutting not in progress" signal, are detected by direct comparison of the appropriate input voltages with the constraint limit voltages. The detection process consists of analog comparison, threshold detection, and logic inversion where necessary.

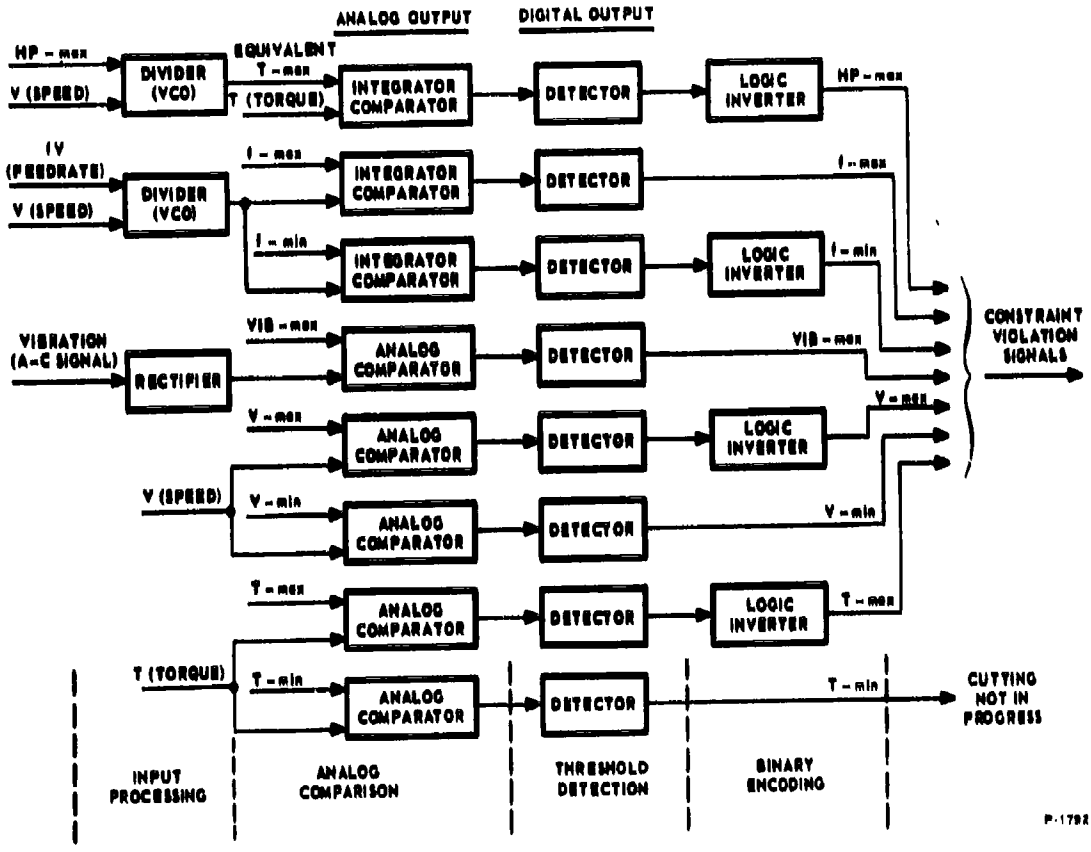


Figure 2-4 - Constraint Violation Detectors

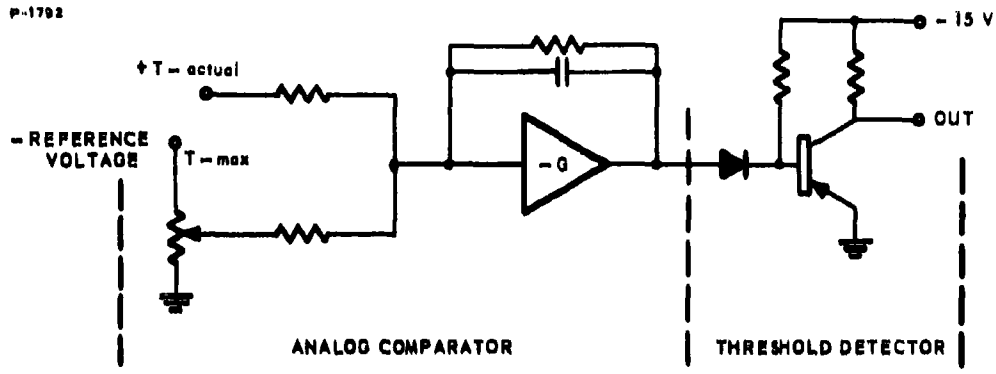


Figure 2-5 - Typical Comparison and Detection Circuit

A typical comparison and detection circuit is illustrated in Figure 2-5. Referring to the figure, a positive d-c voltage proportional to actual torque is one of the inputs to the circuit; this voltage and a negative voltage proportional to the maximum torque limit are supplied as inputs to an operational amplifier, the output of which is applied to a threshold detector. If T-actual > T-max the output voltage will be a large negative value, and if T-actual < T-max (a violation condition) the output voltage will be near zero. In the adaptive controller negative voltages are interpreted as logic "1" and zero voltage as logic "0". To conform to the coding definition given in the first paragraph, it is necessary to logically invert the output of the T-max detector. Identical circuitry is used for the detection of V-max, V-min, T-min and maximum vibration, except that the vibration signal is rectified prior to entering the comparison circuit. In cases where actual output of the threshold circuit conforms to the desired coding, the logic inversion is not required.

Since voltage analogs of horsepower and feed are not directly available to the detector, additional computation is necessary to detect a violation of constraints (1), (5), or (6). Voltage analogs of absolute feedrate, fV, and spindle speed, V, are available, and thus a division operation can be used to compute the feed per revolution, f. A proven analog divider circuit which has been used in previous Bendix systems is available. This circuit, which is known as a VCO (voltage-controlled oscillator), produces an output pulse train having a frequency proportional to the quotient of two d-c input voltages. By applying d-c voltages proportional to fV and V to a VCO circuit, an output frequency directly proportional to f is obtained. To determine if f is within limits,

the time average value of the pulse train is effectively compared to a d-c voltage proportional to the limiting value. This is accomplished by integrating the instantaneous sum of the d-c voltage and the pulse train. The output of the integrator-comparator circuit is then applied to a threshold detector circuit identical to that shown in Figure 2-5. The same technique is used for both feed constraints, (5) and (6).

The voltage analog of horsepower is not computed. Instead the maximum horsepower constraint voltage is divided by the speed, using the VCO technique, to obtain a normalized maximum value. This normalized value has the units of torque and is compared to the actual torque to determine if the horsepower constraint has been violated.

During Phase II a brief test program was conducted to verify the performance of the constraint violation detector circuitry. The system tested included a VCO divider, integrator-comparator, and threshold detector. The major points of operation that were tested included response time, hysteresis, and linearity between actual input voltages and constraint limit voltages. The test results were satisfactory in all respects. It was found that the output of the system would indicate a constraint violation within 10 milliseconds after an appropriate change in the input. The hysteresis of the system is defined as the smallest percent change of the input voltage needed to cause triggering of the threshold detector. This was measured to be less than 2 percent of the input voltage over the full range of operation. It was also verified that the linearity of the system was quite adequate for this application.

### 2.2.4 Performance Computer

This subsystem produces the figure of merit, H, given by

$$H = \left| \frac{MRR}{K_1 + \left( \frac{K_1 \tau + K_2 B}{W_o} \right) \left( TWR_c \right)} \right| \quad 0 \leq B \leq 1$$

The quantities $K_1$ and $(K_1 \tau + K_2 B)/W_o$ are operator-entered constants, while MRR and $TWR_c$ are available as voltage analogs from the data reduction subsystem. The computation is accomplished in three successive steps, as shown in Figure 2-6. $TWR_c$ is multiplied by $(K_1 \tau + K_2 B)/W_o$ and then added to $K_1$ to form the denominator of the figure of the merit equation. This is divided into MRR using the

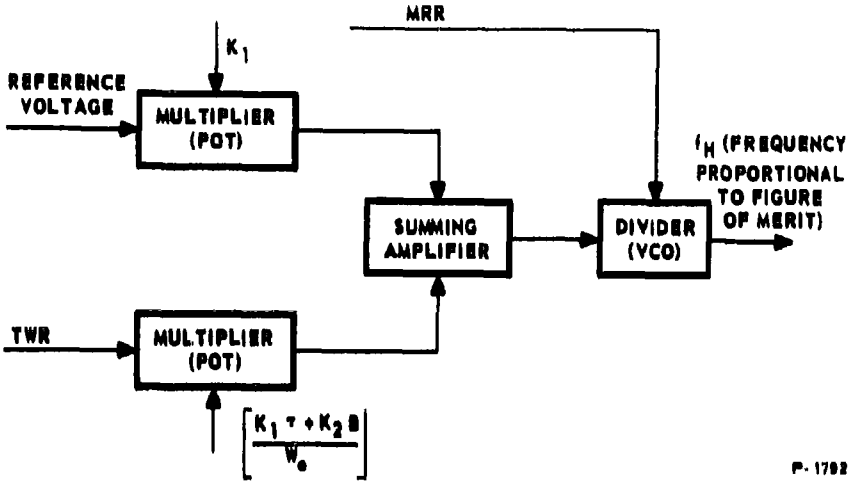


Figure 2-6 - Block Diagram of Performance Computer

above-mentioned VCO circuit as a divider. The VCO output pulse train $f_H$ has a frequency directly proportional to the figure of merit. This pulse train is presented directly to the optimization computer, which effectively performs a digital integration to determine the value of H.

### 2.2.5 Optimization Computer

The primary function of the optimization computer is the execution of the optimizing strategy. A secondary function is to correct any constraint violations that may occur. The optimization computer receives the seven binary coded constraint violation signals from the data reduction subsystem, and a pulse train of frequency proportional to the figure of merit H from the performance computer. The outputs are binary representations of a feed correction increment, $\Delta f$, and a speed correction increment, $\Delta V$. The entire operation is digital in nature.

#### 2.2.5.1 Optimizing Strategy

The strategy employed is basically the method of steepest ascent which was described in the Phase I final report. This is a hill-climbing operation in which the hill is ascended in the direction of steepest slope. The strategy begins with an exploration of the response surface in the region of the starting point to determine a local gradient. The operating point is then moved a single step in the direction of this gradient. A new local gradient is calculated after this single

step, and the operating point is shifted accordingly. This cycle is repeated until the peak of the hill is reached, with the step size modified periodically according to various criteria.

The above procedure has been modified somewhat for use in the adaptive controller. The initial exploration consists of moving one unit ($K_f$) in the ± f direction, observing the response change $\Delta H_1$, moving one unit ($K_V$) in the ± V direction, and observing the response change $\Delta H_2$. The next move consists simply of incrementing f by $K_3 \Delta H_1$ (observing sign) and incrementing V by $K_4 \Delta H_2$, where $K_3$ and $K_4$ are scale-factor constants. The result is that the gradient has been approximated and the operating point moved in the direction of this approximate gradient with a step size proportional to its magnitude. Thus a continuous step size adjustment is effected. Figure 2-7 illustrates this procedure for a typical response surface. Note that each major (gradient) movement of the operating point is preceded by two smaller (exploratory) movements along the f and V axes. It may also be noted that the gradient move is always nearly normal to the constant H-value contours.

Execution of the steepest ascent strategy is accomplished by straightforward digital techniques. The logical sequence diagram of the procedure is illustrated in Figure 2-8. Each of the three major operations within the cycle requires a fixed amount of time, known as the sampling period. It is presently believed that a sampling period of 0.08 seconds is a reasonable value; thus a total of 0.24 seconds would be required to complete the entire sequence. The initial model of the adaptive controller will have provision for manual adjustment of the sampling period to enable experimental determination of the best value. The sequence diagram is self-explanatory with the exception of the effects of constraint violations, which are discussed in the following section. The quantity $\Delta H_1$ is the response of the figure of merit to an exploratory move in feed, and the quantity $\Delta H_2$ is the response to an exploratory move in speed. $K_f$ and $K_V$ are manually set constants which control the size of the corresponding exploratory moves, and $K_3$ and $K_4$ are constants which control the scale factors of the gradient move. The quantities A and B

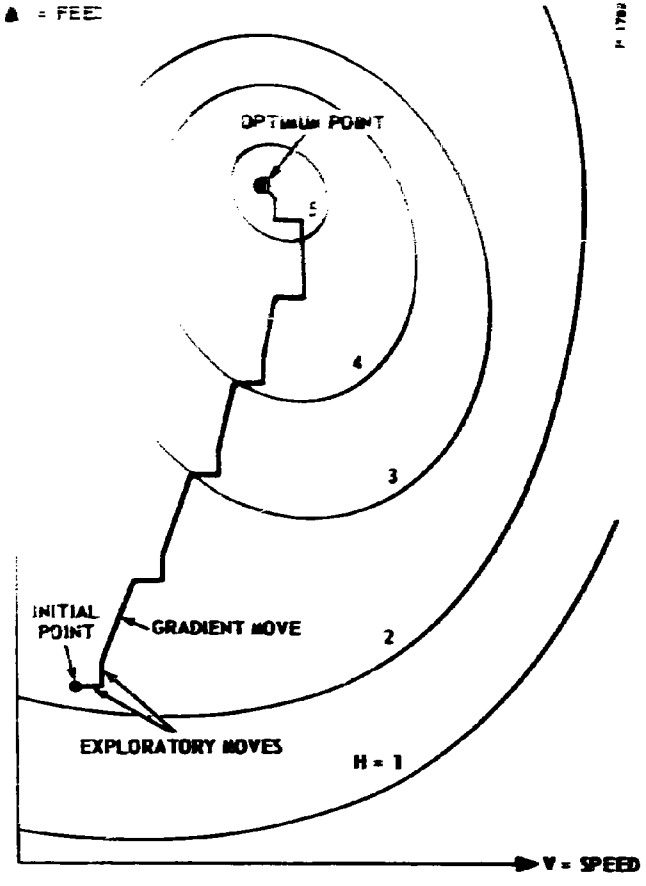


Figure 2-7 - Illustration of Steepest Ascent Strategy

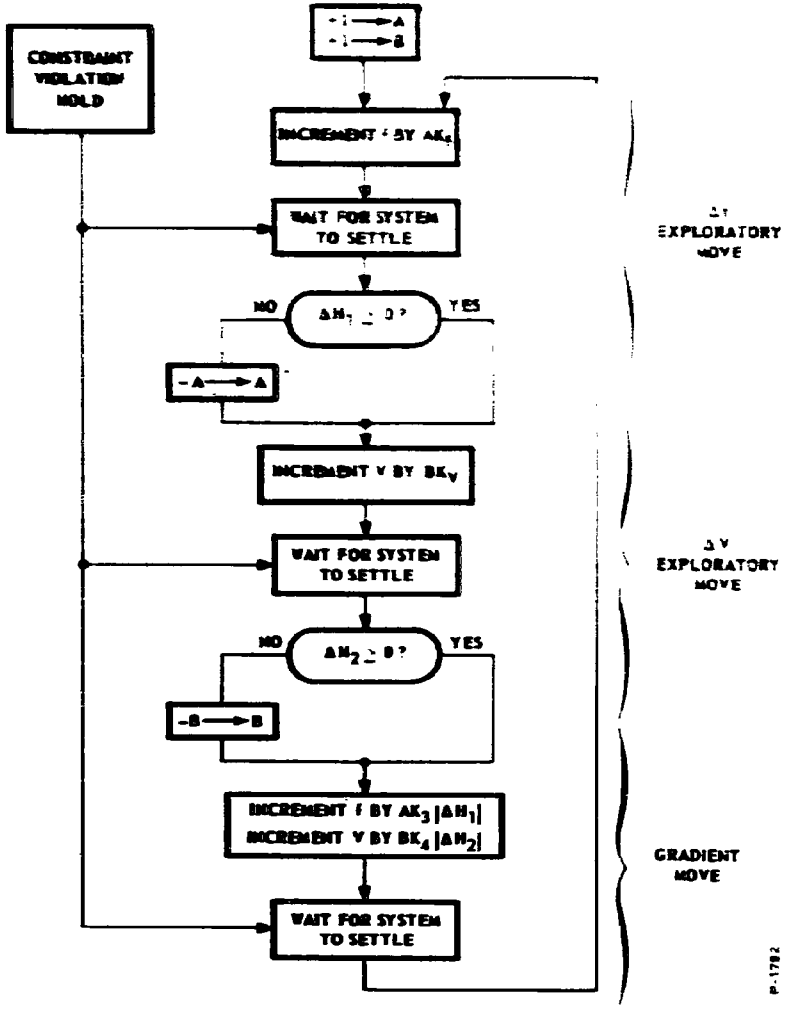


Figure 2-8 - Steepest Ascent Strategy Sequence Diagram

have a value of +1 or -1, and indicate the sign of the exploratory moves and of the f and V components of the gradient move.*

Figure 2-9 is a block diagram of the optimization computer. The programmer receives synchronization signals from the numerical control system and in turn directs the timing of the strategy logic and the constraint violation logic.

The figure of merit is presented to the optimization computer as a train of pulses, $f_H$, the frequency of which is proportional to H. Let $H_1$ be defined as the value of H just prior to an exploratory move. Measurement of $H_1$ consists of opening the sample gate for a fixed period of time and accumulating the $H_1$ pulses into the up counter. During the exploratory move the $H_1$ value is transferred

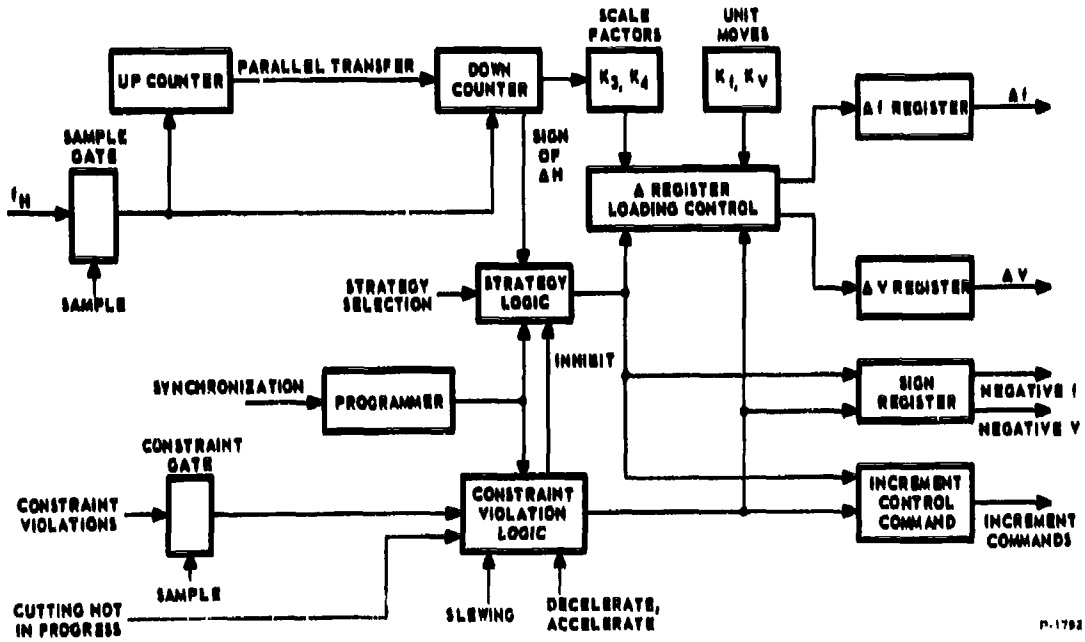


Figure 2-9 - Block Diagram of Optimization Computer

*Note that the signs of the exploratory moves are not constant, but are changed if they move the operating point away from the optimum. It may also be noted that by deletion of the gradient move a trial-and-error strategy may be effected. Since there is little additional hardware required, a strategy selection switch will be included to enable testing of both strategies.

in parallel to the down counter. After the exploration has been completed, a new figure of merit value $H_2$ exists. The $H_2$ pulses are used to decrement the $H_1$ value stored in the down counter for the same fixed time period. The remainder in the down counter is thus

$$\Delta H_1 = H_1 - H_2 \quad .$$

At the same time as the $H_2$ pulses are decreasing the number stored in the down counter they are accumulated in the up counter for use in the computation of $\Delta H_2$. This process is repeated before and after each exploratory move.

The down counter is so constructed that both $\Delta H$ and $-\Delta H$ (complemented form) are available as outputs. Also, information concerning the sign of $\Delta H$ is supplied to the strategy logic. The strategy logic will then select the appropriate output such that $|\Delta H|$ is always used. The gradient move scale factor constants $K_3$ and $K_4$ are integer powers of two. Multiplying $\Delta H$ by these values consists of shifting the bits of $\Delta H$ one or more bit spaces to the right or left.

Referring to Figure 2-9, the $\Delta$ register loading control has four channels of input information: $K_3|\Delta H_1|$, $K_4|\Delta H_2|$, $K_f$, and $K_V$. Upon command from the strategy logic, appropriate channels are connected to the $\Delta f$ or $\Delta V$ registers, and the proper numbers are transferred into the registers. The $K_f$ and $K_V$ values are entered by means of binary coded toggle switches. The numbers stored in the $\Delta f$ and $\Delta V$ registers may represent either exploratory move values or gradient move values, depending upon the particular operation in progress. A two bit sign register is loaded by the strategy logic at the same time as the $\Delta f$ and $\Delta V$ registers. These two bits, A and B, indicate the signs of the quantities in the $\Delta$ registers, and are taken from a storage section in the strategy logic. After the $\Delta f$ and $\Delta V$ registers have been loaded, the strategy logic will issue an "execute increment" command. Separate commands are given for f increments and for V increments. Both commands are given for the gradient move. The execute commands are transmitted to the numerical control system interface and used to initiate the process of correcting the feed and speed values in accordance with the contents of the $\Delta f$ and $\Delta V$ registers.

### 2.2.5.2 Constraint Violation Logic

At regular intervals the constraint violation logic opens the constraint gate and examines the outputs from the constraint

violation detectors. Immediately upon detection of a violation the optimizing strategy is inhibited and the controller is shifted into a special correction subroutine. The correction commands given by the constraint violation logic are similar to the strategy commands. The constraint violation logic activates the $\Delta$ register loading control, loads the sign register, and gives "execute increment" commands as required. The following correction rules are used.

| VIOLATION | CORRECTION |
|---|---|
| HP-max | decrease V by $K_V$ |
| VIB-max | decrease V by $K_V$ |
| V-max | decrease V by $K_V$ |
| V-min | increase V by $K_V$ |
| f-max | decrease f by $K_f$ |
| f-min | increase f by $K_f$ |
| T-max | decrease f by $K_f$ |

The correction is repeated until the violation signal is removed. In case of simultaneous occurrence of two violations, e.g., T-max and f-min, the logic is arranged so that the decreasing correction dominates. Also, since f and V corrections may be initiated simultaneously (as in a gradient move), there are no indeterminate or ambiguous conditions.

If the system were returned to the normal optimizing mode as soon as the constraint violation was removed, an unstable limit cycle may result. This would occur if the optimizing strategy immediately returned the system to the previous feed and speed values which resulted in the constraint violation. To preclude the occurrence of the limit cycle, a specially modified optimization logic is used immediately after removing a constraint violation. The special logic prohibits the immediate repetition of the moves which led to the violation condition. A further discussion of this problem is included in Appendix II.

Receipt of a "cutting not in progress" signal from the data reduction subsystem will simulate a constraint violation and thereby inhibit the optimizing strategy. However, no corrective action will be taken. The feed and speed commands within the numerical control system will then hold their present value until the signal is

removed, indicating that cutting has resumed. Indication of slewing or decelerating/accelerating conditions from the numerical control system will have the same effect on the optimization computer. However, the deceleration and acceleration will be implemented within the numerical control system in such a manner as to maintain relatively constant chip load.

### 2.2.6 Numerical Control System Interface

The parameters to be adjusted by the adaptive controller are spindle speed and absolute feedrate. The commands for these quantities are stored in the numerical control system in serial binary form on magnetostrictive delay lines. The desired incremental change in spindle speed, $\Delta V$, is available directly from the adaptive controller and thus a serial add-subtract technique can be used to modify the stored spindle speed command. However, the absolute feedrate F is equal to the product of f and V, and $\Delta F$ is not directly available. Therefore a special computation is required. The numerical control system interface includes the circuitry required to implement this computation plus the timing and control circuitry necessary to synchronize the adaptive controller outputs with the numerical control system logic. Figure 2-10 is a block diagram of the interface logic. When no increments are being supplied by the adaptive controller, the interface logic simply circulates the present values of V and f through the input control logic.

When an execute increment command is received, the interface programmer is started. The programmer supplies the timing and control signals necessary for the interface arithmetic. Operation is best illustrated for the gradient move, where both f and V increments are present. Let $f_{in}$ and $V_{in}$ be the initial values of f and V. The first step is the updating of $f_{in}$. The input control logic closes the recirculate path to $f_{in}$ and applies $f_{in}$ to the X input of the adder-subtractor. At the same time $\Delta f$ is serialized and applied to the Y input, and the sign of $\Delta f$ is applied through the sign logic. The output of the adder-subtractor is $(f_{in} \pm \Delta f)$, which is sent by the output control to the feed storage delay line and to the multiplier. Similarly, $V_{in}$ is updated and $(V_{in} \pm \Delta V)$ is applied to the multiplier. The outputs of the interface are thus

$$V_{out} = V_{in} \pm \Delta V$$

and

$$F_{out} = (f_{in} \pm \Delta f)\ (V_{in} \pm \Delta V)$$

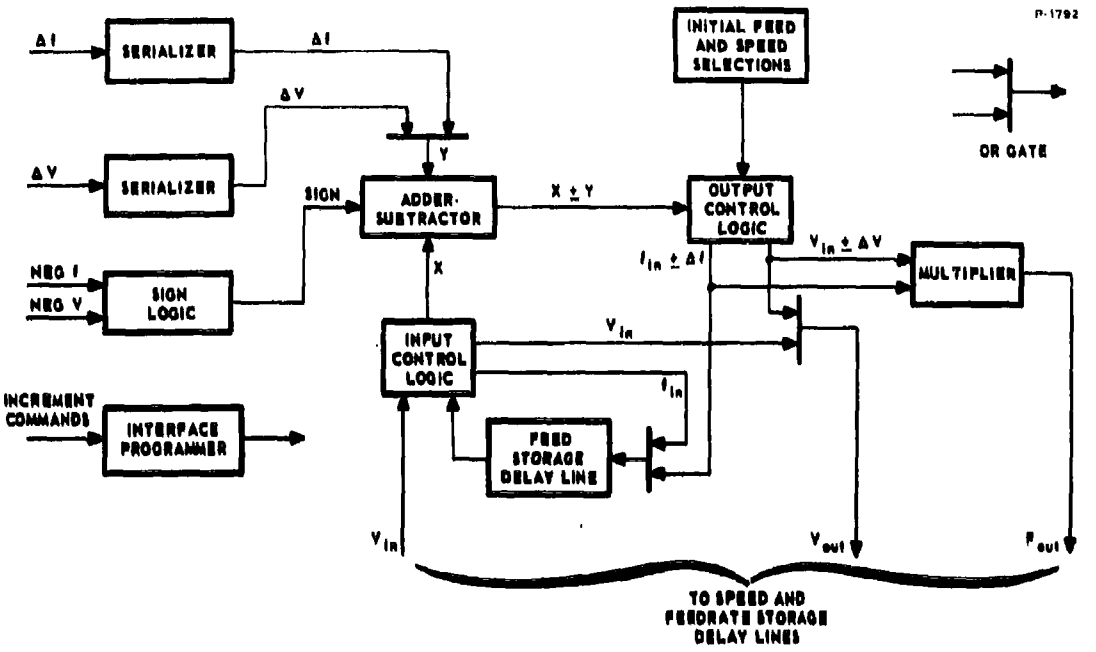


Figure 2-10 - Block Diagram of Numerical Control System Interface

For the exploratory or constraint increments $\Delta f$ or $\Delta V$ may be zero but the operation of the interface logic is identical.

### 2.2.7 Simulation Study

A computer simulation study of the closed loop adaptive control system was performed during Phase II. The objectives of this simulation study were:

(1) to compare the convergence capabilities of both a gradient and a trial-and-error strategy in the presence of noise and operating point drift;

(2) to compare the drift-following capabilities of the above two strategies once an optimum operating point had been reached;

(3) to examine the stability of the closed loop system;

(4) to determine the effectiveness of the constraint violation logic.

The study was performed on an IBM 650 digital computer. Twenty-six simulated runs were made for which the tool-work interface constants were chosen to represent the following workpiece, cutter, and cut geometry:

| | |
|---|---|
| Workpiece: | Carbon steel, Brinell hardness = 300 |
| Cutter: | Carbide, 4 teeth, 1 inch diameter |
| Cut: | Depth = 1/8 inch, width = 1 inch |

Different combinations of feed and speed setpoints, constraint limits, drift, and noise were used in different runs in order to test various features of the adaptive controller logic. The base of the figure of m merit, B, was chosen equal to 1.0 for most of the runs, so that the strategy functioned to minimize the cost per piece. Cost constants were selected to be typical for a numerically controlled milling operation.

The simulation study is described in detail in Appendix II, which also includes a number of figures illustrating the performance of the simulated system. The results of the study are summarized briefly in the paragraphs below.

The initial results of the simulation study indicated poor convergence capabilities of each strategy under certain conditions. Modification of the strategy logic corrected this situation, and it was subsequently concluded that, for a general response surface, the gradient strategy (method of steepest ascent) is superior to the trial-and-error strategy. For the simulated cases, convergence was obtained in 50 to 250 individual moves, including both gradient and exploratory moves. The actual time required per move will be a function of the process dynamics and the response times of the feed and speed servos. A conservative assumption of 0.080 seconds per move would yield convergence in 4 to 20 seconds. (In the actual system, the sampling rate will be increased to the highest usable value to minimize the system response time.) The simulation results also verified that the steepest ascent strategy could function adequately in the presence of both drift and noise.

Simulations of the constraint violation logic disclosed a potential instability involving a limit-cycle between the constraint logic and the optimizing strategy. Refinement of the constraint violation correction rules eliminated this possibility, and the constraint logic then functioned effectively in all but certain very isolated cases.

## 2.3 EXPERIMENTAL METALCUTTING PROGRAM

The general objective of the Phase II experimental metalcutting program was to develop instrumentation to continuously monitor the cutting performance of a numerically controlled milling machine. Instrumentation was developed to measure cutting torque, average tool-tip temperature, and tool vibration for a range of spindle velocities and feedrates. Attempts were made to correlate the measured variables with tool wear rate and workpiece surface finish in order to establish functional relationships for use by the adaptive controller. The program was carried out on a numerically controlled milling machine, using a standard two-inch, four-tooth end-mill cutter with inserted carbide tips. The principle workpiece material was annealed AISI 4140 steel.

The experimental program began on 11 February 1963, and ended on 28 June 1963,after approximately 2,000 test cuts had been completed. Each test cut was twenty-four inches in length and one-half inch in width. The bulk of the program effort was about equally divided between gathering experimental data and development of cutting performance instrumentation. The measurement of spindle torque proved to be the most difficult and time-consuming to implement satisfactorily.

This section is primarily concerned with a summary of the results achieved during the Phase II portion of the experimental program. A brief description of the experimental setup is given in Section 2.3.1, followed by a summary of the test program in Section 2.3.2. A detailed analysis of the test results is given in Section 2.3.3, followed by conclusions to date in Section 2.3.4 and recommendations for future work in Section 2.3.5.

### 2.3.1 Experimental Setup

The experimental metalcutting program was carried out on a Pratt and Whitney Keller three-spindle milling machine. An overall view of the experimental setup is shown in Figure 2-11. The lower spindle was modified by replacing the normal spindle drive motor with a variable speed hydraulic motor. The modification included a special rear bearing cap and a hydraulic drive motor with a manifold mounted servo valve. The hydraulic motor was driven by a specially installed hydraulic power supply that was capable of driving the spindle motor over a speed range of zero to 2000 rpm. Early in the program it was

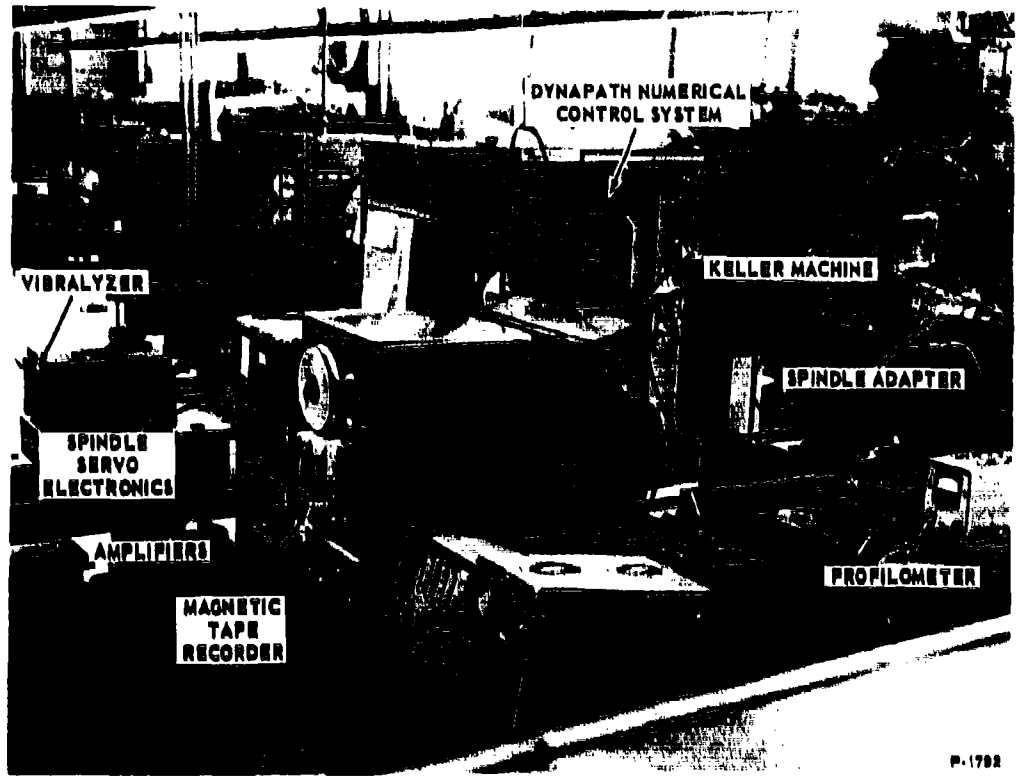


Figure 2-11 - Overall View of Experimental Setup

found necessary to close a velocity servo loop around the spindle drive system, using a tachometer feedback. In the open-loop mode the spindle velocity was overly sensitive to load, causing erratic variations in the performance data.

The measurement of cutting torque and average tool-tip temperature was accomplished by means of an instrumented spindle adapter mounted in place of the standard tool holder on the lower spindle of the milling machine. Figure 2-12 shows a close-up view of the adapter and illustrates a test cut being made on the 4140 steel. RayData Corporation of Columbus, Ohio, designed and fabricated the instrumented adapter. The adapter contains a flexure element in line with the cutting tool and a low-noise slip ring assembly with gold plated brushes and rings. Figure 2-13 shows the internal flexure element and the slip rings. Torsional strain was measured by semiconductor strain gages

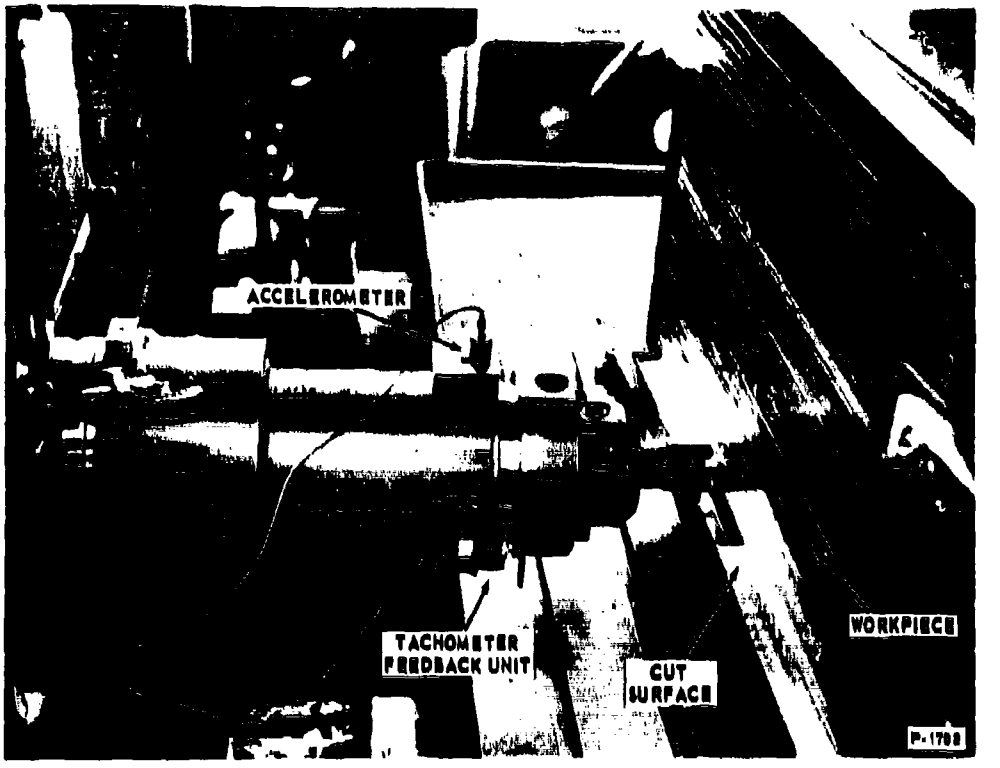


Figure 2-12 - Close-up View of Instrumented Spindle Adapter

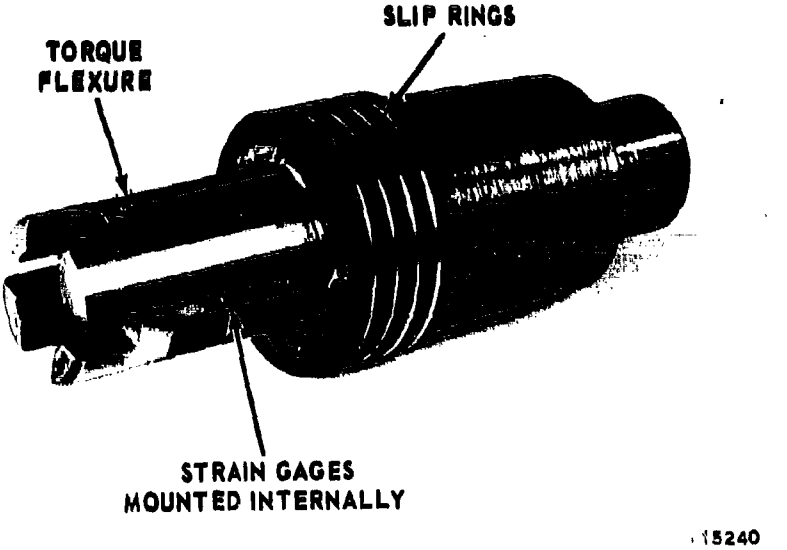


Figure 2-13 - Torque [illegible] S[illegible] Rings

cemented to both ends of an arm in the flexure element. The strain gage and tool temperature leads were brought out through the slip ring assembly.

The average tool-tip temperature was measured by a technique that uses the cutting tool and the workpiece junction as a thermocouple. The technique is based on the fact that any two dissimilar metals, when in contact, will generate an electromotive force (emf). The amplitude of the emf is a function of the temperature at the contact point. The measurement of tool vibration was accomplished by means of a crystal accelerometer mounted on the instrumented spindle adapter near the cutting tool. Actual spindle speed was monitored by means of a magnetic pickup mounted on the adapter. A digital counter was used to count the magnetic pulses which were simultaneously displayed on an oscilloscope.

During the experimental test runs, all sensor signals were continuously monitored on a dual beam oscilloscope, using the differential inputs to both beams of the oscilloscope. For post-test analysis, the torque, temperature, vibration, and spindle velocity were recorded on magnetic tape by means of a Sanborn/Ampex Model 2000 multi-channel magnetic tape recorder. Each channel of this recorder could be set to either FM or direct recording. The cutting torque and temperature signals were recorded on FM channels, and the accelerometer and magnetic velocity pickup signals were recorded on the direct channels. A Kay Electric Vibralyzer instrument was used in the post-test analysis of tool vibration signals.

Wear land measurements were made optically using a X50 microscope with a reticle ruled scale having 0.001 inch divisions; estimates to 0.0005 inches could be made. The surface finish of the workpiece was recorded by means of a Profilometer gage manufactured by Micrometrical Manufacturing Company. The tracer pickup arm of the Profilometer limited the width of the test cuts to a minimum of 0.5 inch.

A detailed description of the experimental setup and the sensors is given in Appendix I.

### 2.3.2 Summary of Test Program

The experimental program was carried out for the process of peripheral milling using a climb cut. In this type of milling, the

intermittent cutting action between the rotating cutter and slowly moving workpiece takes place on the outer periphery of the cutter, and the thickness of the chip formed decreases from an initial maximum as the cut progresses. The cutters used during the tests were heavy duty two-inch diameter end mills with inserted carbide tips. The 4140 steel workpiece was 1-1/4 inches thick and 24 by 36 inches in length. To enable use of the thermocouple temperature measuring technique, the workpiece was electrically insulated from the base plate of the milling machine by sheets of masonite.

During initial checkout and calibration of the instrumentation, it became evident that the strain-gage torque bridge was sensitive to bending moments. Consequently, the machine drive system was carefully realigned and the torque flexure was reground to improve concentricity between the machine and adapter. Although this improved the situation, operation was still not satisfactory. The bending moment problem was finally solved by replacing the original pin drive between the machine and the adapter by an Oldham coupling. Initial metalcutting tests also revealed that the peak cutting torques were somewhat higher than had been anticipated. Consequently, the torque design limit of the flexure element was exceeded during some of the early tests. To solve this problem, it was necessary to design and fabricate a stronger torque flexure unit. As a result of these initial instrumentation problems, the start of the actual experimental program was delayed for approximately two months.

After the instrumentation system problems were cleared up, an initial series of runs were made to gain familiarity with the system. Practical ranges of cutting conditions were determined by observing the sensor outputs as a function of feed, speed, and depth of cut. Following the exploratory test runs, a series of planned tests were conducted to gather performance data. The tests consisted of milling a flat strip 24 inches in length and 0.5 inches in width, using various spindle speeds and feedrates. Periodically, the torque, temperature, and vibration were recorded on magnetic tape. At each data point the cutting tool was removed and the wear land was recorded along with the surface finish of the workpiece.

The first series of tests was carried out using a 0.04 inch depth of cut for a combination of three spindle velocities and three feedrates. With only one-third of the tests completed a crack developed in the torque flexure. The crack occurred in the weakest section of the

flexure element between the corner of one of the slots into which the Oldham coupling fit and the nearest rectangular slit between the flexure arms. The adapter was then removed from the milling machine and dismantled. The crack in the flexure element was repaired with an electron beam welder. After the adapter was remounted, a new series of tests were planned at a 0.02 inch depth of cut. The welded flexure element performed satisfactorily throughout the remainder of the Phase II program.

The tests all began with a sharp cutter ground with a primary relief angle of six degrees. Each time a specified volume of metal had been cut, the tool was removed from the machine and the wear land of each tooth was measured at a point 0.070 inches from the tool-tip. Surface finish measurements were then made with the Profilometer. The tests were terminated either when the spindle torque approached the design limit of the instrumentation system or when the wear land reached a value of 0.025 inch. A further description of the tests that were run and a detailed analysis of the results is contained in the next section.

### 2.3.3 Summary of Results

This section summarizes the analytical results of the experimental program, which consisted of climb milling 4140 steel using a carbide tipped cutter under the following conditions:

| | |
|---|---|
| Cutting velocity: | 525 to 950 feet per minute |
| Feed per tooth: | 0.0018 to 0.0072 inch |
| Depth of cut: | 0.020, 0.040 inch |
| Width of cut: | 0.5 inch |

The analysis of data obtained during the program was directed towards establishing functional relations between the measurable variables, temperature, torque, and vibration, and the metalcutting performance factors. Particular emphasis was placed upon development of a technique to enable on-line determination of tool wear rate (TWR), and upon determination of the constraints required to guarantee the production of an acceptable part. The general approach was to abstract information from the measured data which correlated reasonably with the milling performance factors and upon which a practical controller could be based, rather than to attempt verification of the theoretical mechanisms actually occurring during metalcutting.

#### 2.3.3.1 Metal Removal Rate

The rate at which metal is removed from the workpiece, MRR, is given by:

$$MRR = Fwd$$

where the terms are defined in Section 2.2.3. The width and depth are programmed values, and a signal proportional to the actual feedrate, F, is available within the numerical control system. Thus MRR can be obtained without the need for any sensor information. However, if the actual depth of cut deviates from its programmed value as a result of lateral deflection of the cutting tool, the MRR calculation will be incorrect. Such deviation of depth is especially likely in the case of very light cuts where there is insufficient force at the cutting edge to penetrate the workpiece, and the cutter tends to ride along the surface.

Control of the depth of cut during the experimental program was achieved by automatic advance of the cutting tool by the distance, d, after each pass at the workpiece. This automatic advance was under control of the DynaPath unit, and was independent of the actual amount of metal removed during previous passes. Thus any reduction of actual depth due to tool deflection would result in a build-up of the workpiece surface relative to the tool on succeeding passes, and would cause uneven and erratic cutting as the penetration of the cutter varied from cut to cut. A study of the torque signal indicated that such erratic cutting did not take place over the range of cutting conditions used in the test program. This was further confirmed by visual inspection of the chips produced, and it was therefore concluded that the depth of cut was insignificantly affected by tool deflection.

#### 2.3.3.2 Tool Wear Rate

A sharp cutting tool was installed at the beginning of each test, and wear measurements were made at periodic intervals during the test. The tool was retired and the test concluded when either a maximum wear land on the order of 0.025 inch was observed, or when the peak torque approached the allowable limit of the instrumentation system. The only type of wear which was experienced throughout the program was the formation of a rather even wear land on the clearance face of the tool. Wear of the rake face (cratering) was never observed. Figure 2-14(a) is a photograph of a tool-tip which was used for milling

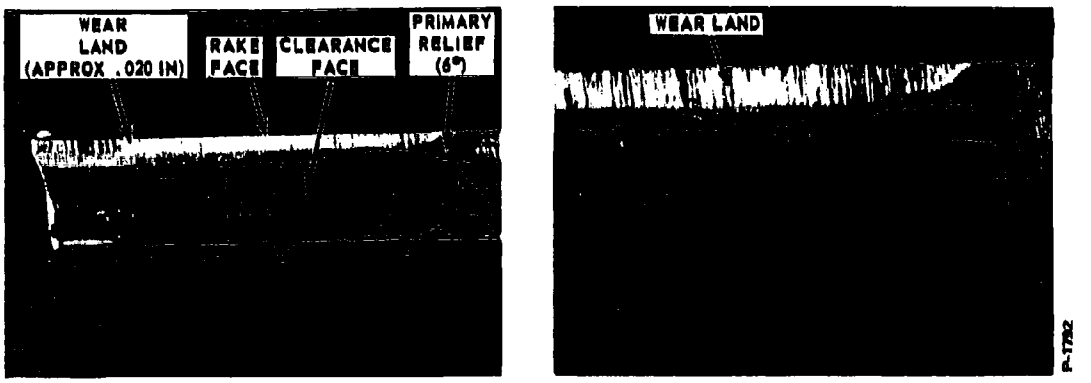


a. MAGNIFICATION X 6 b. MAGNIFICATION X 13

Figure 2-14 - Tool Tip Showing Typical Wear Formation

4140 steel showing the typical wear land formation. Figure 2-14(b) is an enlarged section of the same photograph.

During initial tests a four-tooth cutter was used, and it was observed that the tool-tip extremities were not perfectly concentric with the center of spindle rotation. This gave rise to an equivalent tool-tip runout which, by mechanical adjustment, could be reduced to approximately 0.002 inch for the worst tooth. In an effort to eliminate runout effects, as well as to obtain wear data more rapidly, three cutter tips were removed and data was taken using the resultant one-tooth cutter. Data analysis indicated this to be a reasonable approach, since the one-tooth wear data correlated fairly well with the four-tooth-averaged data of a four-tooth cutter.

Figure 2-15 is a plot of wear vs. cutting time for several typical runs. All of the curves obtained are characterized by a period of initial rapid wear averaging approximately 30 minutes during which "break in" occurred, followed by a period of reduced, almost constant wear rate for the bulk of the remaining tool life. In addition, some of the wear plots contain a period of increasing wear rate near the end of the tool life. These curves are of the same form as those obtained by Shaw and Dirke.[2]

An oscilloscope trace of the amplified signal obtained from the tool-work thermocouple is shown in Figure 2-16. Typically, the peak thermocouple voltage was initially low, and it

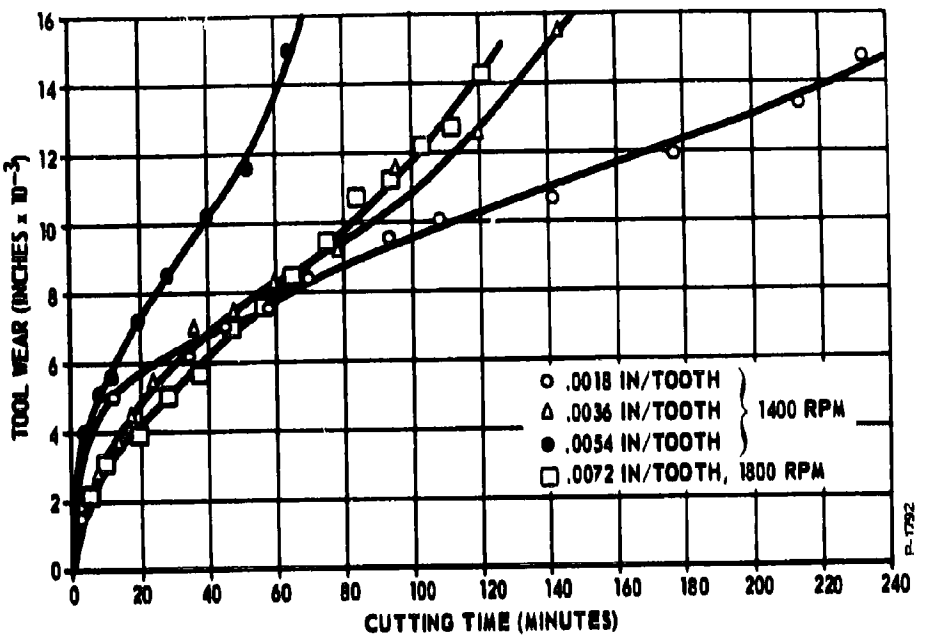


Figure 2-15 - Tool Wear vs Cutting Time for a Series of Tests

increased on the order of 10 percent during the progress of a single test (with feed and speed constant). Although this voltage did not correlate with the actual value of the tool wear rate at a specific instant of time during any single test run, it was related to the average value of wear rate from run to run. Thus, the peak thermocouple voltage was sensitive to changes in tool wear rate as a function of feed and speed, but not as a function of time. This may be seen from Figures 2-17 and 2-18 showing, respectively, instantaneous TWR and peak thermocouple voltage vs. time for a single run, and average TWR vs. average peak thermocouple voltage for a series of runs.

A typical torque waveform is shown in Figure 2-19. The peak torque increased by a factor of from two to three times its initial value during the progress of a single test run. Although only slight correlation was obtained between the actual torque magnitude and TWR, a greater correlation was noted between the rate of change of peak torque and TWR. Specifically, the torque rate was sensitive to changes in TWR with time during individual test runs. An exception to this is that the initial rapid wear of the tool which occurred during break-in was not accompanied by a correspondingly large torque

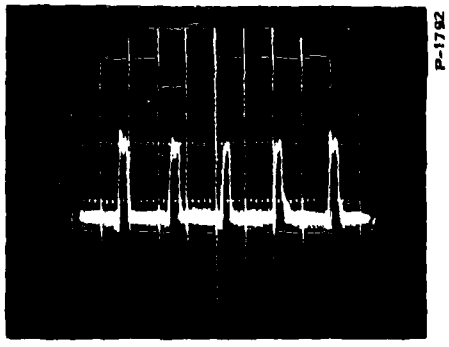


VERTICAL SCALE = 0.2 V/CM
HORIZONTAL SCALE = 5 MS/CM
(AMPLIFIER GAIN = 50)

Figure 2-16 - Amplified Signal from Tool-Work Thermocouple

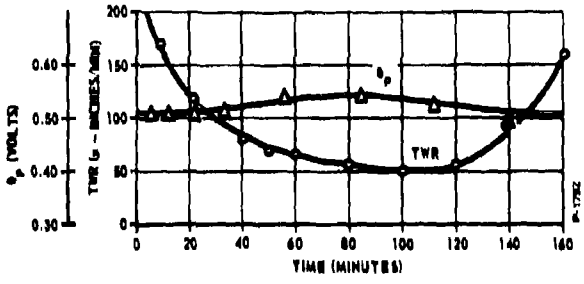


Figure 2-17 - Instantaneous $\theta_p$ and TWR vs. Time for a Typical Test Run

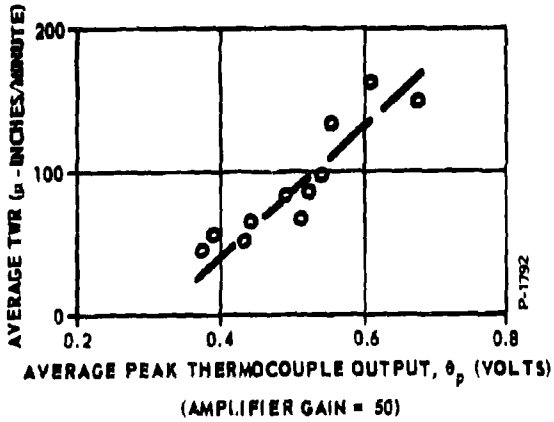


(AMPLIFIER GAIN = 50)

Figure 2-18 - Average TWR vs. Average $\theta_p$ for a Series of Tests

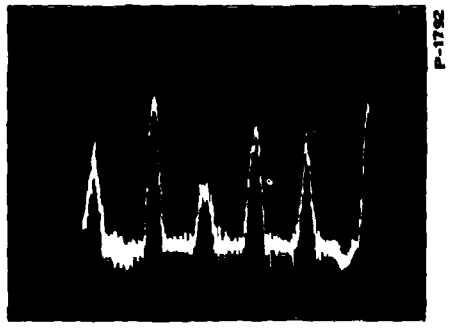


VERTICAL SCALE = 0.5 V/CM
HORIZONTAL SCALE = 5 MS/CM
TORQUE SCALE FACTOR = 318 IN-LB/V

Figure 2-19 - Typical Torque Signal

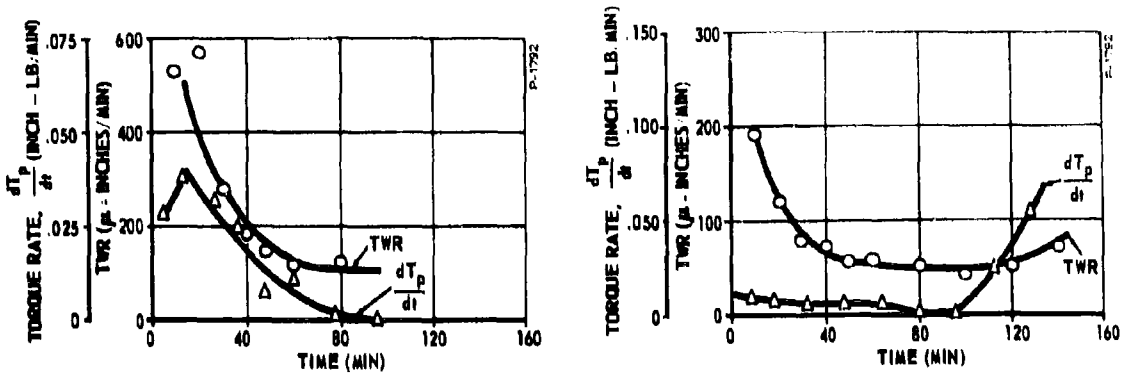


Figure 2-20 - Torque Rate and TWR vs Time for Two Typical Tests

rate value. Figure 2-20 shows TWR and torque rate vs. time for two test runs. The calculated values of torque rate which were used in the analysis were based upon torque differences over rather large periods of time (orders of minutes), and as such represent long term torque rate averages. It is probable that better correlation could be obtained by using a shorter term rate average.

In addition to TWR correlation with thermocouple voltage and torque rate, it was found that a reasonable correlation with MRR existed. Since MRR was held constant throughout each individual test run, it was insensitive to changes in instantaneous TWR over the run. It was observed, however, that MRR could be related to the average TWR over a given test run. Figure 2-21 is a plot of MRR vs. average TWR for a series of runs.

Use has been made of the above correlations to establish a curve fit of the instantaneous TWR data accumulated over the entire test program. A linear approximation of the following form was chosen.

$$TWR_c = K_5\ MRR + K_6\ \theta_p + K_7\ \frac{dT_p}{dt}$$

where

$TWR_c$ = calculated tool wear rate (in/min)

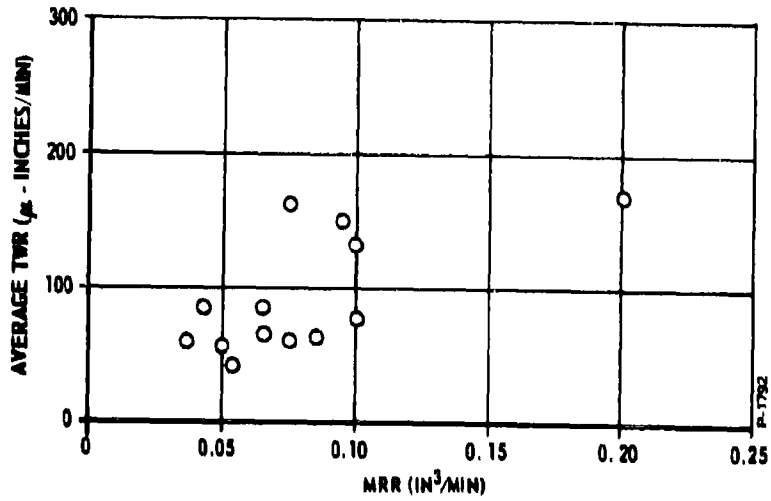


Figure 2-21 - Average TWR vs MRR for a Series of Tests

$K_5 = 0.63$ $(in^{-2})$

$K_6 = 0.063$ $(in/min\text{-}volt)$ } Weighting Factors

$K_7 = 0.0028$ $(lb^{-1})$

Although this expression is not the most general which could have been chosen, it does fit the data reasonably well and has the obvious advantage of being relatively simple to implement. Furthermore, an approximate error analysis has indicated that this expression will be suitable for use in the adaptive controller. The error analysis is discussed in the following paragraphs.

A comparison of calculated and actual TWR for four typical runs is shown in Figure 2-22. In each of these plots it can be seen that the greatest error occurred during the first 30 minutes of tool life. This was the case for all of the test runs, and is due to the insensitivity of all of the measured parameters to the initial rapid wear of the tool. Since all of these initial errors are fairly consistent, they could be at least partly compensated by inclusion of an additional term in the TWR equation, the magnitude of which would decrease as a function of time. It is not planned to use this approach in the initial model of the adaptive controller, since the slight reduction in overall (integrated) error would not justify the increased hardware and complexity.

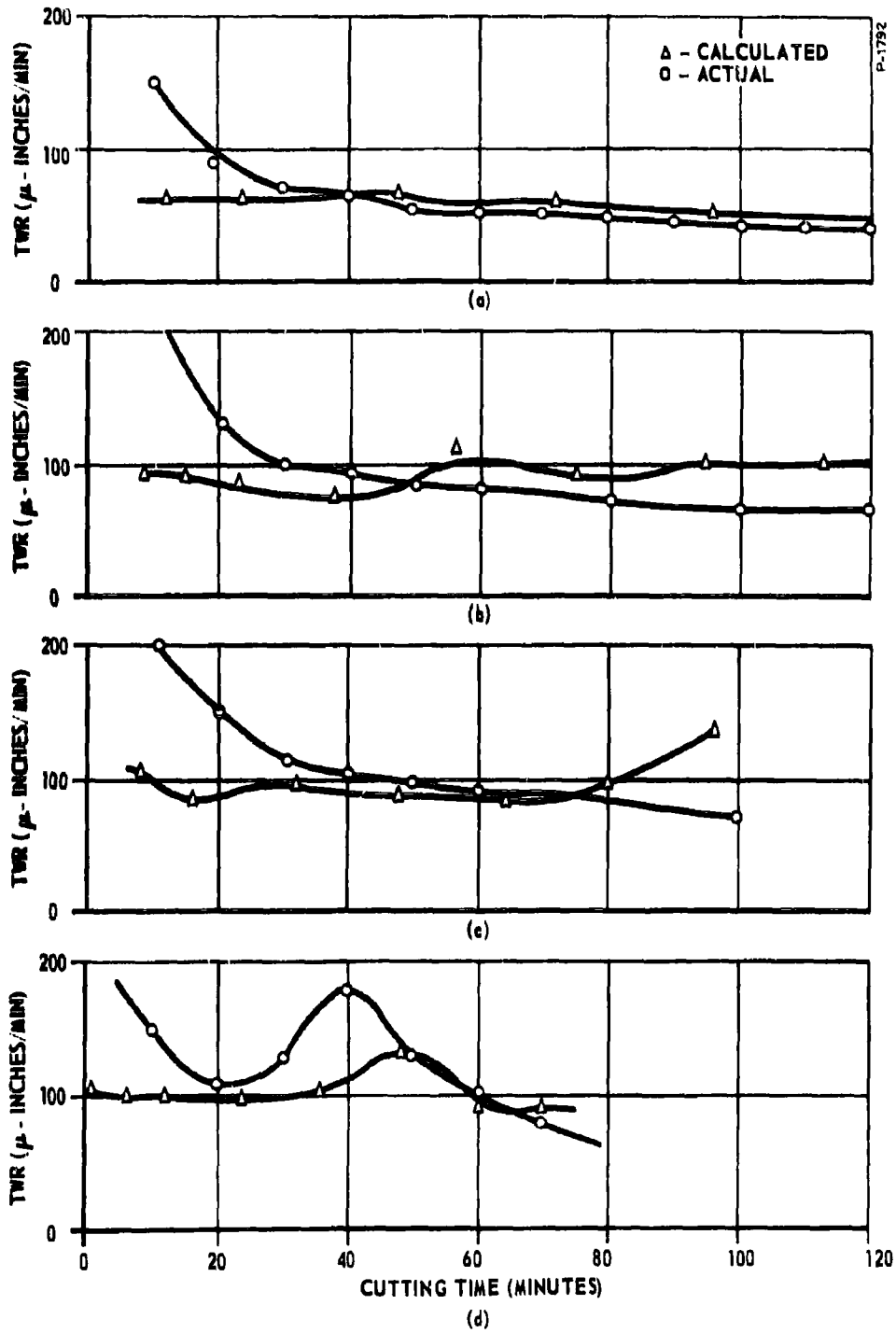


Figure 2-22 - TWR Curve Fits for Four Typical Tests

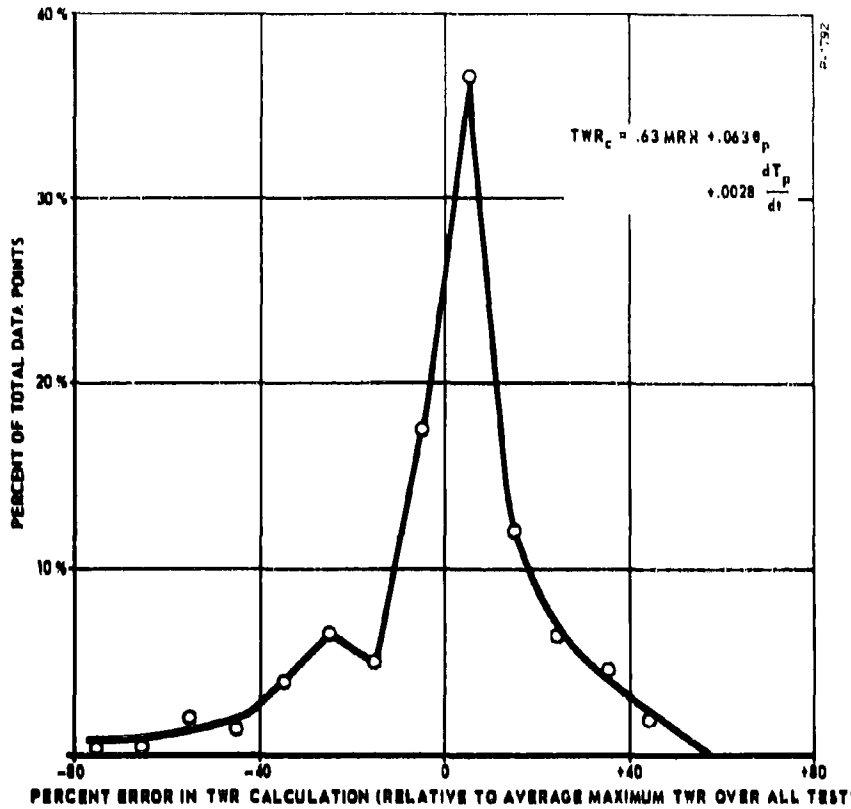


Figure 2-23 - Error Distribution for TWR Linear Approximation

The percent error in the value of $TWR_c$ relative to the average maximum TWR occurring over all of the runs has been tabulated, with calculations being made at each ten minute interval for every test. The distribution of errors is shown in Figure 2-23, and may be summarized as follows:

| Percent of Total Points | Error Band |
|---|---|
| 54% | ± 10% |
| 84% | ± 30% |
| 96% | ± 50% |

It was shown in the Phase I final report that optimum control of the metalcutting process requires maximization of the function,

$$\int H_a \, dt$$

where

$H_a$ = figure of merit based on the actual tool wear rate, TWR

It is thus apparent that to minimize the effect of errors, the following integral must be minimized:

$$\int \left| H_a - H_c \right| dt$$

where

$H_c$ = figure of merit based on $TWR_c$

This is equivalent to minimizing,

$$\int \left| TWR - TWR_c \right| dt$$

which may be used as a criterion for evaluating various curve fits to the TWR data.

The actual degradation of overall system performance caused by a given error in $TWR_c$ cannot be directly calculated in cubic inches per dollar, since it is a function of the actual figure of merit response surface. This in turn is determined by the function relating TWR to feed and speed, as well as by choice of the cost constants $K_1$ and $K_2$. The effect of such an error is to create an apparent response surface which is different in shape and magnitude from the true response surface, as illustrated in Figure 2-24. The adaptive controller is forced to work with the apparent response surface and it therefore acts to maximize the quantity $H_c$ by adjustment of feed and speed values. In reality, the apparently optimized values of feed and speed correspond to a value of $H_a$ on the true response surface which is less than optimum.

It is apparent from a study of the figure of merit equation that the effect of errors in $TWR_c$ will be greatly reduced if

$$K_1 >> \left[ \frac{K_1 \tau + K_2 B}{W_o} \right] (TWR)$$

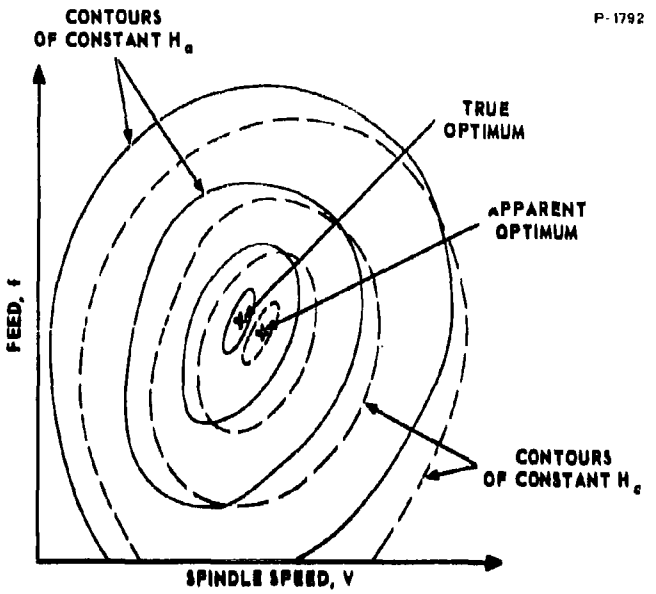


Figure 2-24 - Effect of Error in $TWR_c$ on Hypothetical Response Surface

This inequality will generally be true for a typical numerically controlled milling operation where the value of direct labor plus overhead rate, $K_1$, is likely to be rather high compared to the tooling cost per unit time, $K_2$. To determine the actual effect of $TWR_c$ errors for a typical set of constants, use was made of the closed-loop system simulation as described in Appendix II. The constants used are given in Table II-1. Various errors in $TWR_c$ were assumed and the simulated controller was allowed to establish an operating point at the apparent optimum. The results are summarized below:

| Error in $TWR_c$ | Value of Apparent Optimum ($in^3/\$$) | True Value of $H(in^3/\$)$ | |
|---|---|---|---|
| +25% | 5.1636 | 5.4934 | |
| +10% | 5.3636 | 5.5140 | |
| +05% | 5.4304 | 5.5175 | |
| 0 | -- | 5.5195 | True Optimum |
| -05% | 5.6059 | 5.5189 | |
| -10% | 5.7005 | 5.5149 | |
| -25% | 6.0182 | 5.4716 | |

Thus, for the simulated case an error of ±25 percent in $TWR_C$ resulted in an actual performance degradation of less than ±1 percent.

### 2.3.3.3 Constraints

The experimental data has been analyzed in an attempt to determine a basis for establishing suitable constraint limits. The purpose of these limits is to insure that acceptable parts are produced, and also to protect the milling machine from overloads or other undesirable conditions. Maintaining adequate surface finish of the part is of particular importance, and to this end an analysis of the vibration signal was undertaken.


Figure 2-25 - Oscilloscope Trace of Typical Vibration Signal

Figure 2-25 shows an oscilloscope trace of a typical vibration signal as obtained from a crystal accelerometer. Although it has been shown by other investigators that surface finish data may be extracted from vibration signals in milling,[3] little success was achieved in correlating the amplitude of the composite waveform with surface microfinish as measured with a Profilometer

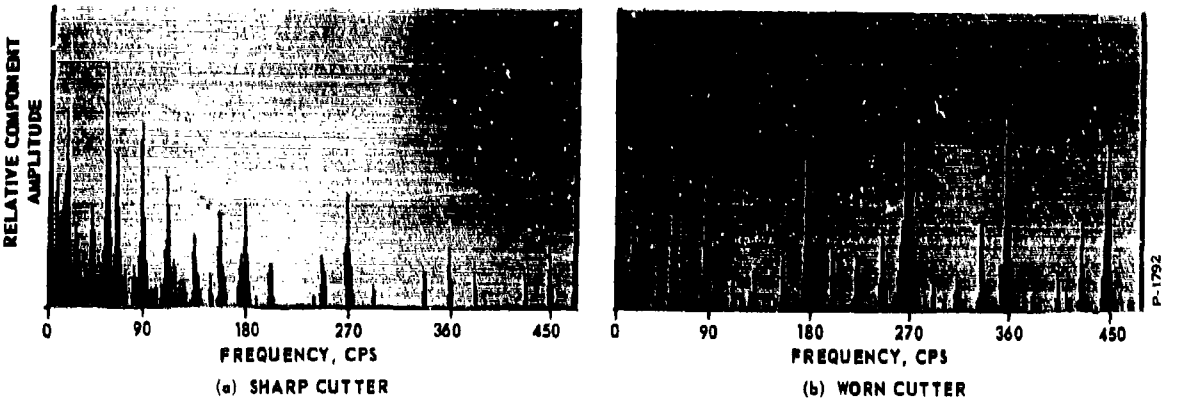


Figure 2-26 - Frequency Spectrum of Vibration Signal

gage. It is believed that pertinent information may have been lost in attempting to characterize the surface finish with a single rms micro-inch number, and that future analysis would be aided by using a device able to record the actual surface profile. Frequency spectra of the vibration signals were obtained using a Kay Electric Vibralyzer. Examples of the amplitude vs. frequency plots obtained with the Vibralyzer are shown in Figure 2-26(a). This plot, which is the vibration spectrum immediately after installation of a sharp tool, indicates main frequency components at 20, 60, and 90 cps. In general, it has been found that low frequency components dominate initially, and that as the tool wears the spectrum spreads out and higher frequency components tend to dominate. This effect is illustrated by Figure 2-26(b) which shows the spectrum under the same conditions as (a) except that the tool is considerably worn. Here the main components center around 270 cps. It has also been observed that for some of the tests the surface finish deteriorates as the tool wears. Thus, the data suggests the possibility of a relation existing between surface microfinish and the frequencies of the main components of the vibration signal. To date, however, such a correlation has not been definitely established.

Feed marks in the surface were not measured quantitatively, but their presence was confirmed by visual inspection of the workpiece. These marks can be geometrically determined from the values of feed per tooth and depth of cut. A maximum feed constraint may be determined as a result of limitations placed on the size of these feed marks.

The maximum torque limit can be established on the basis of structual or dimensional accuracy limitations, whichever is more stringent. In the Phase II experimental setup the torque flexure limitation would clearly establish the T-max limit.

To date it appears that the maximum horsepower limit should be set on the basis of the spindle drive limitation, since there has been little indication that horsepower correlates with workpiece quality. The remaining limits, on feed and speed, should be set as liberally as possible to allow the controller maximum freedom of adjustment.

#### 2.3.3.4 Stainless Steel Workpiece Material

In addition to the tests run with 4140 steel workpiece material, some experimentation was carried out using type

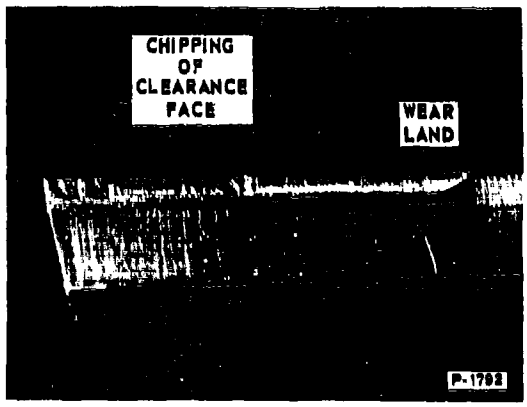


Figure 2-27 - Tool Tip Showing Chipped Clearance Face

AMS 5639A stainless steel with the same cutter. In this case, excessive chipping of the clearance face was experienced as shown in Figure 2-27. It was therefore concluded that the cutter geometry was inappropriate for this workpiece material. Due to time limitations, it was decided to forego further tests on the stainless steel in Phase II and to return to this workpiece material in Phase III, after sufficient data was accumulated for the 4140 steel.

### 2.3.4 Conclusions to Date

A large body of data for the machining of 4140 steel has been accumulated and analyzed. It has been verified that tool deflections materially affecting the depth of cut did not occur, and that the computed value of MRR is thus a valid one. Tool wear rate data has been correlated with MRR, torque rate, and tool-work thermocouple voltage, and a linear approximation to the tool wear rate as a function of these variables has been established. It has been shown that the expected errors in this approximation should degrade the overall controller performance only slightly, and this has been verified by computer simulation. The applicability of the linear approximation to widely varying cutting conditions and to different workpiece materials has not been determined as yet. It has been concluded that the linear approximation is adequate under the conditions of the Phase II experimental program and therefore it will be used in the initial model of the adaptive controller.

Little success was achieved in attempting to correlate surface microfinish with the vibration signal. Both the composite vibration waveform and its frequency spectrum were considered in the analysis. It is suspected that information was lost by using a simple rms microfinish measurement. Also, the spindle adapter maximum torque limitation degraded the validity of the analysis somewhat, since chatter conditions could not be obtained and all microfinish measurements indicated values of less than 200 microinch rms. Present design of the adaptive controller includes a constraint on maximum vibration

amplitude. Refinements of this feature will be incorporated as more is learned of the relation between microfinish and vibration.

Sufficient information has been obtained during the experimental program to justify the presence of the remaining constraints and to establish reasonable limiting values for the various parameters to be constrained.

### 2.3.5 Recommendations for Additional Experimental Work

The following recommendations are made specifically for the Phase III experimental program:

#### (1) New Spindle Instrumentation System

The spindle adapter used for the Phase II metalcutting program should be replaced by an improved device incorporating the following features:

(a) Elimination of auxiliary spindle bearings;

(b) No significant decrease in the basic rigidity of the spindle;

(c) Reduction of the distance from the front spindle bearing to the cutting edges;

(d) Improved compensation against the effects of bending loads;

(e) Increased design margins in all critical areas.

Two different approaches have been conceived to meet the above requirements. One relatively simple method is to mount a four-arm strain gage bridge directly on the spindle. This method would require the use of high-sensitivity semiconductor strain gages with careful attention to temperature and bending compensation. Its major advantages are simplicity and the fact that the spindle dynamics would be practically unaffected by the instrumentation.

The second method would use a new type of spindle adapter, which is illustrated in Figure 2-28 with its members shown shaded. The principle involved is analogous to the use of a shunt circuit to measure high electric currents. In this design all but a small fraction of the cutter torque is taken through a torsion bar which is coupled to the machine spindle through a spline on the left and to the tool holder through

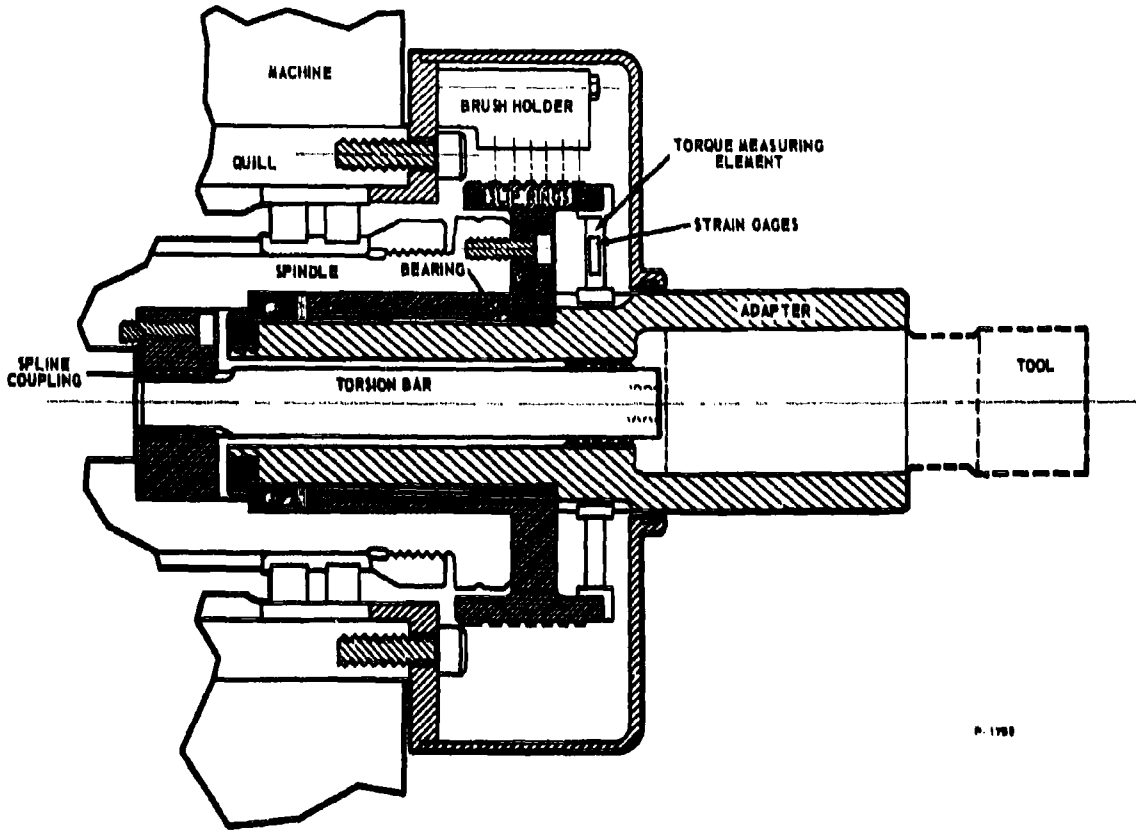


Figure 2-28 - Cross-Sectional Diagram of Proposed Spindle Adapter

a spline on the right. This permits the torsion bar to be conservatively designed, since its stress is not in the measuring loop. The measured torque fraction is taken through a path which includes a strain gage element and is in parallel with the torsion bar. Thus, by changing the cross section of the bar, the measured fraction of the total torque can be changed as may be desired for experimental purposes. In the design shown the torsion bar can be removed and replaced simply by removing the cutter and pulling with a jack screw. Nothing else is disturbed and a simple one-point calibration is sufficient.

Either of the above-described instrumentation techniques would permit the cutter to be mounted with the same overhang normally obtained with an unmodified machine. Thus, the basic rigidity would be essentially unchanged.

(2) Additional Tool Wear Rate Tests

A new series of tests should be run using 4140 steel and a new spindle instrumentation system. The purpose of these tests would be to verify the validity of the TWR curve fit over the wide range of conditions which the new system would permit. Specifically, the depth of cut should be increased to provide data on rough cuts, and the width of cut increased to include the entire thickness of the workpiece material. This latter condition would eliminate physical contact of the cutting tool end with the workpiece and would thus improve the quality of the thermocouple signal by preventing tool-workpiece shorting of the thermal emf.

(3) Additional Surface Finish Tests

It is recommended that a set of tests be run using 4140 steel and the new instrumentation system, specifically for the purpose of isolating surface finish data. This would enable the tests to be designed with a single purpose in mind, and should result in accumulation of more meaningful data. In addition, the new instrumentation system will allow a more practical range of conditions which should include the occurrence of chatter. An instrument capable of recording the true surface profile should be used in these tests.*

The following tests are recommended, but are not considered essential to this project:

(4) Tests with Stainless Steel

Tests should be run with a stainless steel in order to accumulate and analyze both TWR and surface finish data. This would allow comparison of data on different workpiece materials and would indicate changes which might be required to allow the controller to handle a broad class of materials.

(5) Broader Tests with 4140 Steel

A number of tests should be run on 4140 steel to determine the ease with which new cutting configurations can be handled. Included should be tests using conventional cutting, slotting, and a variety of depths and widths of cut. Also, the effects of coolant should be investigated.

---

*Two examples of such instruments are the Proficorder (Micrometrical Mfg. Co.) and the Surficorder (Brush Instruments).

# SECTION 3

# PLANS FOR PHASE III

The work to be accomplished during Phase III of this project includes fabrication, assembly, and initial checkout of the first model of the adaptive control system. In addition, it includes additional experimental metalcutting work in accordance with the recommendations that were given in Section 2.3.5.

## 3.1 SCHEDULE

A schedule for the planned Phase III program is shown in Figure 3-1. As indicated, the total time to complete this phase will be approximately six months. The various activities shown on the chart are discussed in further detail in the following sections.

## 3.2 ADAPTIVE CONTROLLER FABRICATION AND CHECKOUT

Fabrication of the initial model of the adaptive controller will begin at the start of Phase III. A large portion of the fabrication will consist of interwiring between the circuit card modules. All of the parts required for this task were ordered and received during Phase II; therefore the module wiring may begin immediately. Purchase orders will be issued early in Phase III for the additional parts required to complete the controller fabrication. It is estimated that fabrication will be completed in about six weeks.

To facilitate checkout, the initial model of the controller will be mounted in an open relay rack. Checkout will proceed on a subsystem basis and will involve all portions of the system except the interface logic. Externally generated timing signals will be used to drive the programmer and tape-recorded sensor signals will be used to drive the data reduction subsystem.

## 3.3 NUMERICAL CONTROL SYSTEM MODIFICATION

A standard DynaPath numerical control unit will be modified for use in the closed loop adaptive system. Automatic feedrate and spindle speed control modules will be added to the unit. The primary modifications will consist of logic and timing changes in these modules to

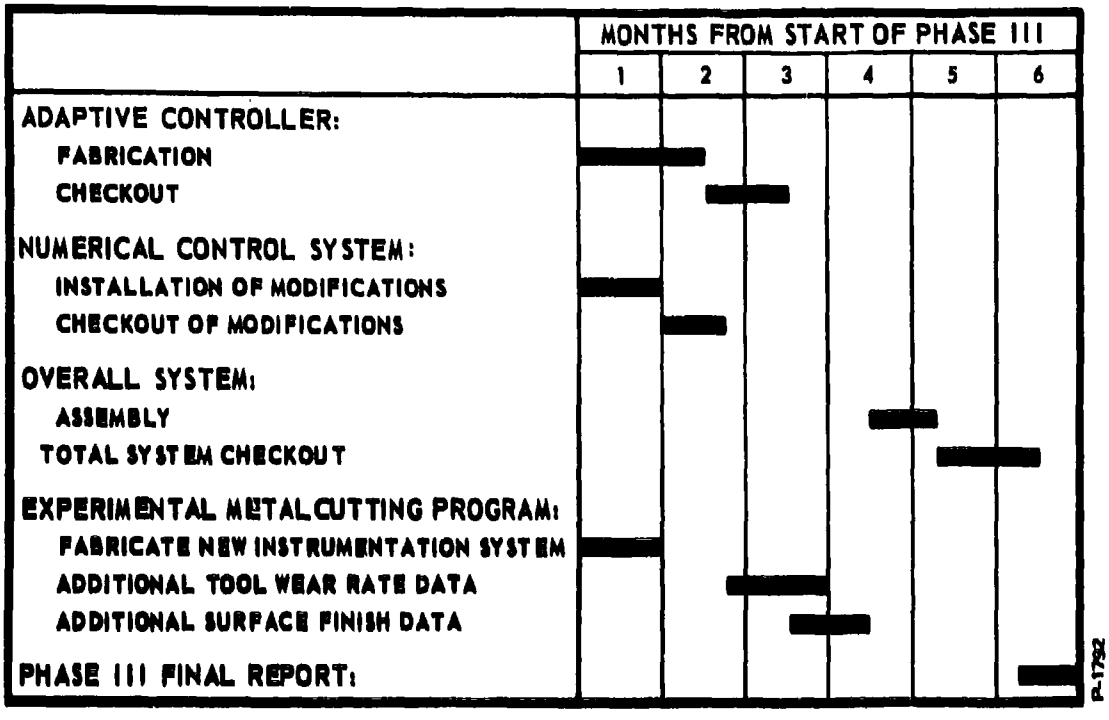


Figure 3-1 - Phase III Schedule

provide a constant chip load feature, and the addition of decoding and storage to accommodate tape-programmed accelerate, decelerate, and slew commands. In addition, the DynaPath delay line circuitry must be modified for compatibility with the adaptive controller interface, and some of the internal DynaPath signals must be buffered for interconnection with the adaptive controller. It is planned to begin these modifications at the start of Phase III and the work is estimated to be complete within one month. Operational checkout of the modified DynaPath unit will then be undertaken.

## 3.4 EXPERIMENTAL PROGRAM

Fabrication of a new spindle instrumentation system is also planned at the start of Phase III. The new system will be based upon one of the methods described in Section 2.3.5. Selection of the particular method will be made after a detailed analysis of the relative merits of the two approaches. After installation of the new system on the machine,

experimental activity will be suspended until the checkout of the modified DynaPath unit is completed. The metalcutting program will then resume. The majority of the program will consist of a series of new tests on 4140 steel and AMS 5639A stainless steel, as recommended in Section 2.3.5. Initial tests will involve the accumulation of tool wear data for both rough and finish cuts for the purpose of verifying the validity of the tool wear rate linear approximation that was developed in Phase II. These will be followed by a series of tests to accumulate surface finish data. A device capable of recording the actual surface profile will be used in this second test series, and data analysis will proceed concurrent with the metalcutting.

## 3.5 ASSEMBLY AND CHECKOUT OF OVERALL SYSTEM

Overall system assembly will begin immediately following the completion of the Phase III experimental metalcutting program. Initial system checkout will consist of open loop tests to verify proper operation of the adaptive controller subsystems. Particular attention will be given to the interface logic. Final checkout will involve closing the loop and confirming proper qualitative operation of all subsystems. The system will be checked for overall stability and for proper functioning of both the constraint violation logic and the strategy logic. A total of two months has been allotted for the combined assembly and checkout of the overall system. Detailed evaluation of the performance of the system is not a portion of Phase III, but will be accomplished during Phase IV.

# SECTION 4

# CONCLUSIONS

The following conclusions can be drawn from the results of the Phase II program.

(a) A simulation study of the complete adaptive control system has indicated that the basic logic design is satisfactory, and that the method of steepest ascent is superior to the trial-and-error approach as an optimizing strategy. The system operation should converge upon feed/speed settings which result in optimum performance, and should be capable of functioning properly in the presence of drift and noise.

(b) All of the data manipulation required in the adaptive controller can be implemented with standard analog and digital electronic circuitry. There is no requirement for development of any special or highly complex circuits.

(c) The adaptive controller can work directly into an existing numerical control system by means of a suitable interface logic. The interface logic is straightforward and should pose no inherent problems.

(d) The instrumentation system used in the Phase II metalcutting program was adequate, but could be improved somewhat. In particular, the spindle torque dynamometer was too limited in maximum allowable torque to enable testing over a wide range of cutting conditions. Other areas in which improvements should be sought include the dynamic response (rigidity) of the torque measuring system, the signal-noise quality of the temperature signal, and the measurement of true surface microfinish. The Profilometer gage used for microfinish measurements is limited in bandwidth and does not provide a true picture of the surface profile.

(e) An empirical equation has been developed for the calculation of tool wear rate as a function of metal removal rate and the measured variables temperature and torque. The validity of this equation has been examined for a large body of data, and it is concluded that the equation is sufficiently accurate for use in the first model of the adaptive control system. The general approach used to obtain this equation is believed to be applicable over a wider range of cutting conditions than was used in the Phase II experimental program.

(f) A set of parameters to be constrained within maximum and/or minimum values has been selected. The purpose of these constraints are to assure production of acceptable parts and to protect the machine and cutter from overloads. Experimental data was used to aid in the selection of these parameters and to determine reasonable values for the maximum and minimum limit settings.

(g) Development of a technique for on-line measurement of surface microfinish will require additional experimental work. The data obtained to date has not shown a significant correlation between the microfinish and any of the measured variables. It is believed that improvements are required in the method of measuring true microfinish, as well as in the processing of tool vibration signals. Until a suitable measurement technique is developed, a constraint on maximum tool vibration amplitude will be used to minimize chatter and thereby maintain at least an upper bound on the microfinish.

(h) The average tool-tip temperature is a key parameter in the on-line measurement of process performance Sensing of this parameter by the tool-work thermocouple technique is feasible without direct connection to the tool-tip, for a carbide tool and 4140 steel workpiece material. Its use for other tool-workpiece combinations would have to be verified experimentally.

# SECTION 5

## RECOMMENDATIONS

Based on the results of Phase II and the conclusions given in Section 4, the following recommendations are made.

(a) The project should be continued through Phase III. The results to date indicate that the basic system concept is sound and that reasonable on-line measurement of a key performance factor, the tool wear rate, is feasible. Consequently there is a high degree of confidence that the adaptive controller will be able to materially improve performance, at least under the cutting conditions tested to date.

(b) The experimental program should be continued, to extend the range of cutting conditions and to develop a technique for on-line measurement of surface microfinish.

(c) A new spindle instrumentation system, using one of the methods described in Section 2.3.5, should be fabricated and used for the remainder of the project. Either of these methods would enable the measurement of high cutting torques, thereby allowing the range of allowable cutting conditions to be expanded.

(d) For surface finish tests, the measurement of actual microfinish should be made with an instrument capable of recording the true surface profile. This would enable direct comparison of the surface profile with the tool vibration signal, which should help to isolate the characteristics of the vibration signal which are related to the true surface finish.

Since tool-tip temperature data was found to be an important parameter in the calculation of tool wear rate, the practicality of this measurement should be further investigated. In the Phase II tests, it was

found possible to obtain satisfactory signals without direct connection of the thermocouple lead to the tool-tip. The approach should be further verified to determine the degree of information loss inherent in this technique. Also, the tool-work thermocouple effect should be investigated for a number of different tool-workpiece combinations to determine its range of applicability.

## BIBLIOGRAPHY


1. Development of Adaptive Control Techniques for Numerically Controlled Milling Machines, Interim Technical Documentary Progress Report Nr. IR I, Contract AF 33(657)-8782, ASD Project Nr. 7-713, The Bendix Corporation, Research Laboratories Division.

2. On the Wear of Cutting Tools, M.C. Shaw and S.O. Dirke, Microtecnic, Volume X, No. 4, 1956.

3. Influence of Vibrations on Tool Life and Surface Condition in Milling Operations, I. H. Opitz, Microtecnic, Volume XII, No. 2.

4. Heat in Metal Cutting, A. O. Schmidt, Machining - Theory and Practice, American Society for Metals, 1950, pp. 239-250.

5. Tool Life Testing, O. W. Boston, Machining - Theory and Practice, American Society for Metals, 1950, pp. 388 - 396.

6. A Study of Optimization Control Techniques, J. M. Idelsohn, Report 2190, The Bendix Corporation, Research Laboratories Division, 1962, p. 15.

# APPENDIX I

## DETAILS OF EXPERIMENTAL SETUP

### MACHINE

The machine used for the test program was a tape-controlled three-spindle Model BL-D Pratt & Whitney Keller. The machine is equipped with a Bendix DynaPath three-axis numerical control system having a pulse value of 0.0002 inches. The lower spindle was modified by replacing the electric spindle motor with a variable speed hydraulic drive system. The hydraulic motor was a Vickers Type 3913 with a manifold mounted servo valve driven by a specially installed hydraulic power supply. The hydraulic power supply was capable of driving the spindle motor over a speed range of zero to 2000 rpm. The hydraulic motor was mounted on a special rear bearing cap in line with the bottom spindle of the machine. A photograph of the machine was shown in Figure 2-11, Section 2.3.1.

### SPINDLE ADAPTER

The instrumented spindle adapter was designed and fabricated by Ray Data Corporation of Columbus, Ohio. Photographs of the adapter were shown in Figures 2-12 and 2-13, Section 2.3.1. A cut-away drawing of the adapter is shown in Figure I-1. The adapter is of a heavy duty construction and mounts on the spindle nose of the milling machine in place of the standard tool holder. The tool holder and cutting tool are mounted on the front end of the unit together with a wire lead fastened to the tool to complete the thermocouple temperature circuit.

The main components in the adapter are a torque flexure element and a slip ring and brush assembly. The flexure and slip ring assembly are an integral part of the drive shaft extending through the center of the adapter. At the front end of the adapter the drive shaft is held by a pair of angular contact bearings mounted to take both thrust and radial loads. All of the cutting torque is transmitted through the flexure section of the shaft. Two semiconductor strain gages are cemented to both ends of one of four arms in the flexure.

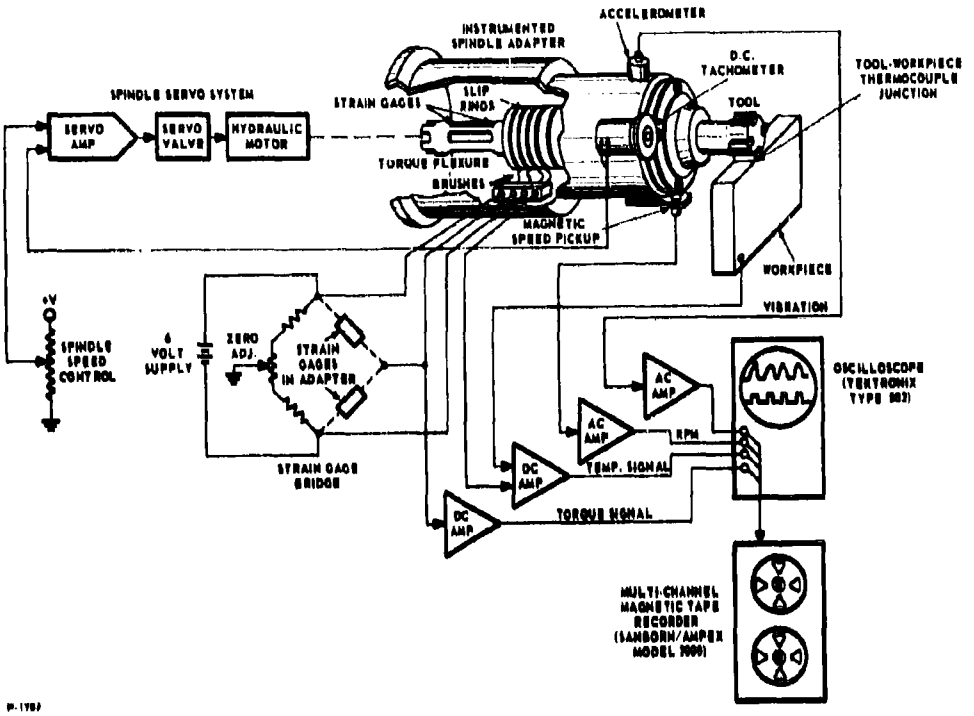


**Figure I-1 - Experimental Metalcutting Instrumentation System**

The slip ring assembly is of a low-noise construction using gold plated rings and brushes. The assembly contains four slip rings; three are connected to the strain gage circuit and one to the cutting tool for completion of the tool-workpiece thermocouple. The slip rings and brushes are completely enclosed by the housing of the adapter to shield the sliding components from metal chips and accidental damage.

## SENSORS

In the experimental program, three sensors were used to monitor the dynamic performance of the peripheral milling process. Cutting torque, average tool-tip temperature, and tool vibration were selected as the measured variables for the program.* These variables were recorded during the metalcutting tests and later analyzed to determine their correlation with the actual performance of the machine. A schematic diagram of the overall instrumentation system is shown in Figure I-1.

---

*The selection of these three quantities was based upon a detailed consideration of the metalcutting literature, plus some preliminary experimentation with other variables such as spindle motor hydraulic pressure and tool deflection.

Cutting torque was measured by means of a strain gage bridge, as shown in the figure. The strain gage elements were cemented to arms of the flexure element in the spindle adapter. Kulite-Bytrex type DB-112 semiconductor strain gages were selected as torque sensors because these silicon gages have a zero temperature coefficient of gage factor when bonded to steel and also have excellent linearity. The DB-112 gages have a nominal resistance of 120 ohms and a gage factor of 58. A torsional strain produced on the flexure element by the cutting action of the tool changes the resistance of the strain gages. The change in resistance is a measure of the cutting torque and is detected by unbalance of the bridge circuit. The strain gage leads are brought out from the flexure element by three slip rings mounted on the drive shaft of the adapter.

Average tool-tip temperature was measured by the tool-workpiece thermocouple method. The tool and workpiece, being dissimilar metals, generate an electromotive force (emf) which is a function of the temperature of their junction. The voltage developed at the junction was amplified by a low-noise d-c amplifier and recorded for analysis. One of the slip rings in the adapter was used to bring out the lead from the tool. Initially the wire was brazed to one tooth in the cutter. However, this proved to be burdensome since the tool had to be removed repeatedly for wear land measurement. After some investigation, it was found that the wire could be fastened directly to the tool holder without noticeably degrading the quality of the temperature signal. The lead at the workpiece was fastened to the metal with a screw and lock washer at the bottom of the steel plate. The tool-workpiece thermocouple was not calibrated for the cutting tests since the absolute measurement accuracy is not critical in this system. It is only necessary to know the correlation between relative changes in thermocouple emf and tool wear.

Tool vibration was measured with a crystal accelerometer mounted on the spindle adapter in the horizontal plane just behind the tool holder. The accelerometer, United Aerotronics Corporation, Model 110-50, had a sensitivity of 28 millivolts per g. A buffer a-c amplifier was used between the accelerometer and the magnetic tape recorder.

## SPINDLE DRIVE SERVO

Performance of the experimental program required a variable speed spindle drive. To accomplish this, the normal 25 hp electric motor in the milling machine was replaced by a Vickers 3913

hydraulic motor. The motor was controlled by a servo valve drive with a power amplifier. Preliminary milling tests with open-loop speed control revealed that the too. velocity would fluctuate as much as thirty percent during a single run. These fluctuations were probably due to hard spots in the steel workpiece. To eliminate this velocity fluctuation, a servo loop was placed around the spindle drive. A d-c tachometer, Servo-Tek Products Company, type SA-740A-2, was mounted on the front end of the adapter. The tachometer shaft was driven with a friction wheel off the rotating tool holder. The output from the tachometer was fed back to the servo amplifier where it was compared with the desired speed control voltage. The spindle drive servo loop is shown in Figure I-1.

## APPENDIX II

## DETAILS OF SIMULATION STUDY

A simulation study of the adaptive control system was performed on an IBM 650 digital computer according to the system block diagram shown in Figure II-1.

The input to the DynaPath Controller is shown to be a feed and a spindle speed command, with initial values f-set and V-set. These initial values are simply setpoints. Feed and spindle servo dynamics were represented by first-order lags having time constants $\tau_1$ and $\tau_2$, respectively. The values of these, as well as other constants employed

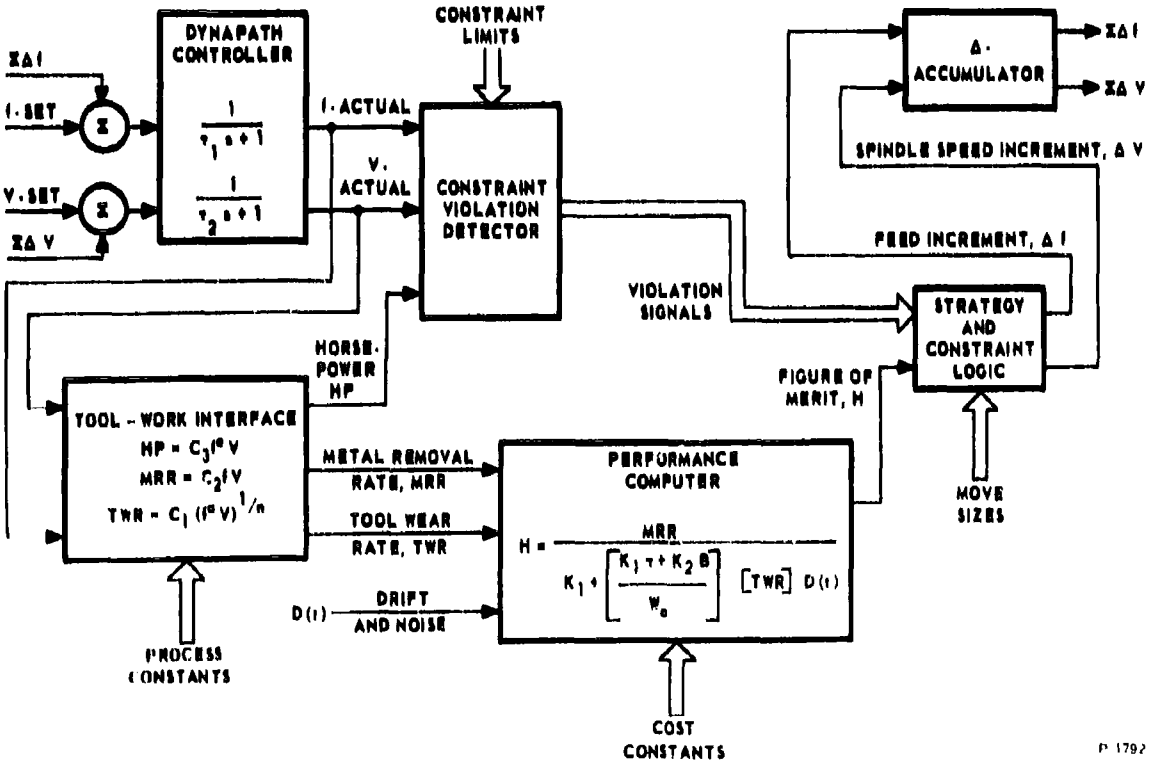


Figure II-1 - Simulation Block Diagram

Table II-1 - Simulation Constants

| | |
|---|---|
| MACHINE | $\tau_1$ = FEED TIME-CONSTANT = 0.025 SEC<br>$\tau_2$ = SPINDLE TIME-CONSTANT = 0.050 SEC |
| TOOL-WORK INTERFACE | TWR = TOOL WEAR RATE (IN/MIN) = $C_1 (f^a V)^{1/n}$<br>$C_1$ = $1.539 \times 10^{-8}$<br>$a$ = 0.8<br>$n$ = 0.3<br>MRR = METAL REMOVAL RATE ($IN^3$/MIN) = $C_2 f V$<br>$C_2$ = 0.128<br>HP = HORSEPOWER = $C_3 f^e V$<br>$C_3$ = 0.14<br>$e$ = 0.9 |
| PERFORMANCE COMPUTER | H = FIGURE OF MERIT = $\dfrac{MRR}{K_1 + \left[\dfrac{K_1 \tau + K_2 B}{W_o}\right] [TWR]\, D(t)}$<br>D(t) = 5% PERIODIC DRIFT OR 0.5% RANDOM NOISE<br>$K_1$ = DIRECT LABOR RATE + OVERHEAD RATE = \$40/HR = \$.67/MIN<br>$\left[\dfrac{K_1 \tau + K_2 B}{W_o}\right]$ = \$378/IN.<br>$K_2$ = COST PER GRIND + $\dfrac{\text{INITIAL TOOL COST}}{\text{MAX. NUMBER OF REGRINDS}}$ = \$10.00<br>$\tau$ = TIME TO CHANGE TOOLS = 2.0 MIN<br>B = BASE OF FIGURE OF MERIT = 1.0<br>$W_o$ = MAX. ALLOWABLE WEAR LAND = 0.030 IN. |
| STRATEGY LOGIC | $K_f$ = $\Delta f$ EXPLORATION = 0.0001 IN/REV<br>$K_V$ = $\Delta V$ EXPLORATION = 10 REV/MIN<br>$K_3$ = $\Delta f$ GRADIENT CONSTANT = 0.01<br>$K_4$ = $\Delta V$ GRADIENT CONSTANT = 1000<br>$T_s$ = STRATEGY MOVE TIME = 0.100 SEC |

R-1792

in the study, are listed in Table II-1. The tool-work interface was simulated using empirical relations obtained from published experimental results.[4] A modified Taylor tool-life expression[5] was used to simulate tool wear rate (TWR), and noise and drift were introduced in the form of perturbations to this quantity.

The simulated adaptive controller consisted of a performance computer, a constraint violation detector, and the strategy and constraint logic as shown in Figure II-1. Rather simple strategy and constraint logic were used during initial runs; subsequently the logic was modified and made more sophisticated for the purpose of improving performance.

Twenty-six simulated runs were made on the computer with the tool-work interface constants chosen to represent the following workpiece, cutter, and cut geometry:

| | |
|---|---|
| Workpiece: | carbon steel, Brinell hardness = 300 |
| Cutter: | carbide, 4 teeth, 1 inch diameter |
| Cut: | depth = 1/8 inch, width = 1 inch |

Different combinations of feed and speed setpoints, constraint limits, drift, and noise were used in different runs in order to test various features of the adaptive controller logic. The base of the figure of merit, B, was chosen equal to 1.0 for most of the runs, so that the strategy functioned to minimize the cost per piece.[1] Cost constants were selected to be typical of a numerically controlled milling operation.

## Convergence of Strategies

As originally conceived, neither the method of steepest ascent (MSA) nor the trial-and-error strategy[6] converged to the optimum feed/speed combination in an efficient manner.

The original MSA strategy consisted of feed and speed exploratory moves, the directions of which were always positive and independent of the response surface. Although the gradient move which followed was in the proper direction for steepest ascent of the surface, it was possible for the progress of this move to be more than offset by the exploratory moves in regions near the optimum point. Thus a true optimum could not always be reached. This situation was corrected by including provision for adjustment of the exploratory move direction such that these moves always tended to aid the progress of the gradient move. The resulting flow diagram for the MSA strategy is that shown in Figure 2-8, Section 2.2.5.

The trial-and-error strategy originally used a step size adjustment criterion which resulted in periodic overshoot past the optimum point and did little to improve the efficiency of the strategy. The flow diagram of the trail-and-error strategy modified to exclude this feature is identical to that of Figure 2-8 with the gradient move deleted.

The response surface or hill which was determined by choice of the various simulation constants is represented by a map of constant figure-of-merit contours as shown in Figure II-2. The hill is ridge-shaped, having a gentle upward slope from lower right to upper left along the ridge, and a rather steep slope on either side of the ridge. Since optimization was with respect to cost, the figure of merit associated with each contour has the units cubic inches per dollar and thus its magnitude is directly proportional to the number of pieces produced per dollar when operating along that contour.

A number of runs were made with both strategies in order to study their convergency capabilities. Results were evaluated by comparing the time required by each for ascent to the optimum operating point, given the same starting point. Since the height of the ridge continuously increases in the positive f direction, operation was limited by a maximum feed constraint at 0.024 inch per revolution to establish a well-defined optimum. Figure II-3 shows plots of runs from three typical starting points for the drift-free and noise-free case. All three runs are shown for the MSA strategy, and one run is shown for the trial-and-error strategy. The other two trial-and-error runs look quite similar to the MSA runs. The results of these runs are summarized below.

| Starting Point | Time for MSA Strategy to Converge | Time for Trial-and-Error Strategy to Converge |
|---|---|---|
| A | 6.9 sec | 6.2 sec |
| B | 11.6 sec | 9.6 sec |
| C | 12.3 sec | 16.4 sec |

It may be noted that the trial-and-error strategy performed more efficiently from starting points A and B, while the MSA strategy did better from point C. This result was as expected, and was caused by the relative ineffectiveness of the gradient move in regions of small slope such as A and B. When allowed to function in regions of steeper slope such as C, the value of the gradient move became apparent. This

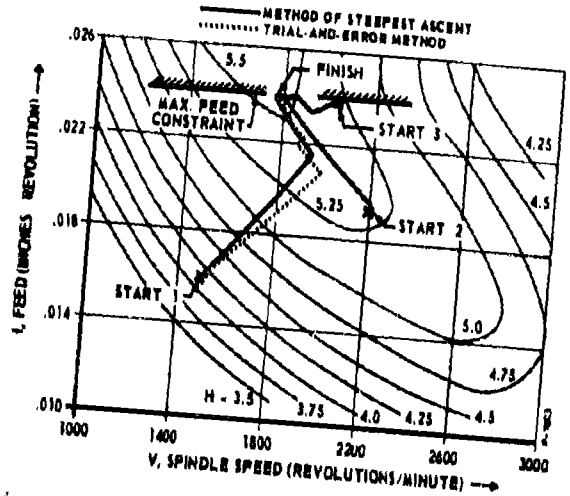


Figure II-2 - Plots of Four Simulated Runs

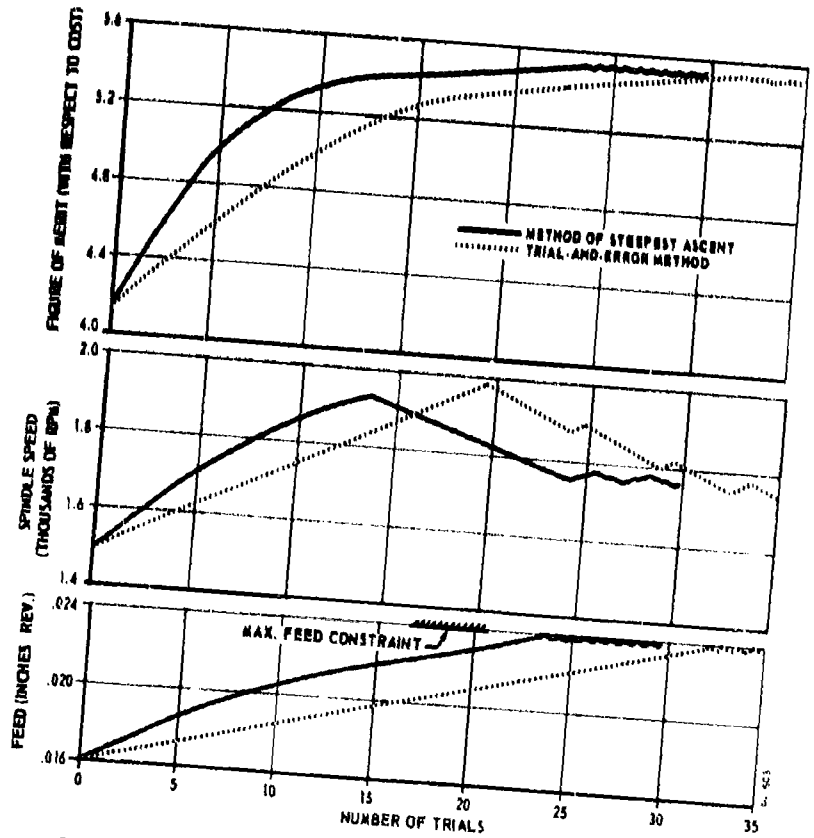


Figure II-3 - Plots of Feed, Speed, and Figure of Merit vs Time

is illustrated by Figure II-3, which shows the progress of each strategy from starting point C as a function of time. The uppermost plot in this figure indicates an initial figure of merit of 4.14 cubic inches of metal removed per dollar, and a final value of 5.42 cubic inches per dollar. These correspond to the setpoint and optimum values respectively, and indicate an over-all cost savings of 31 percent effected by the adaptive controller in this case (this assumes 5.42 to be the average optimum figure of merit).

A more realistic evaluation was made by considering the effects of drift (continuous movement of the peak of the hill) and noise on the ability of each strategy to converge. Although drift and noise would occur simultaneously in the real case, the effects of each were treated separately in the simulation study. Figure II-4 shows the paths followed by each strategy from starting point C in the drift-free case with noise. It can be seen that for trial-and-error strategy, operation proceeded up to the ridge, at which point the strategy became confused by the noise and was no longer able to function properly. The result was that optimization proceeded as if a maximum feed constraint were present at 0.0197 inch per revolution. Figure II-5 shows analogous plots for the noise-free case with drift.* In this case, the trial-and-error strategy

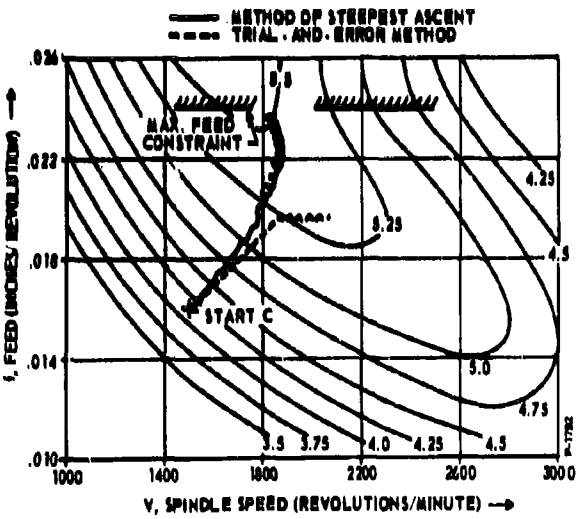


Figure II-4 - Effects of Noise on Strategy Convergence

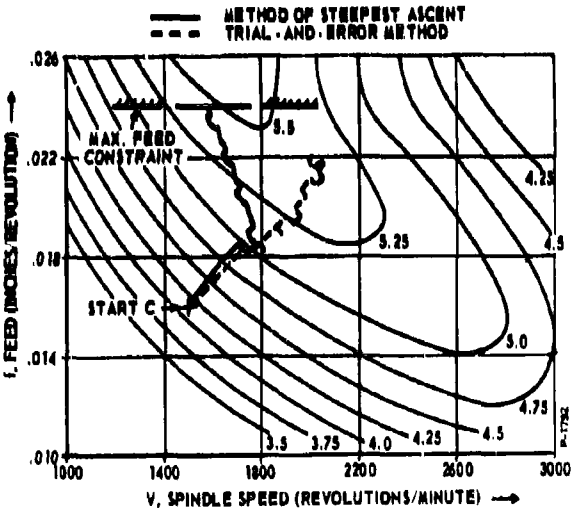


Figure II-5 - Effects of Drift on Strategy Convergence

*The contour map shown is actually the mean map about which the actual map oscillates with a period of 1.05 second.

would ultimately have converged to the optimum point if given sufficient time. The MSA strategy performed satisfactorily in the presence of both drift and noise. The results of these runs are summarized as follows:

| Type of Run | Starting Point | Time for Method of Steepest Ascent to Converge | Time for Trial-and-Error Strategy to Converge |
|---|---|---|---|
| Noise | C | 23.7 sec | Never |
| Drift | C | 23.1 sec | 30.0 + sec |

Drift-Following Capabilities

Consideration was given in the previous section to the effect which drift has on the over-all convergence ability of each strategy. Such an effect may be considered as macroscopic with respect to the adaptive controller. This section deals with the transient, or microscopic effect of drift, and considers the short term capabilities of each strategy to respond to comparatively rapid changes in the process equations.

For small-signal a-c perturbations of the milling process, the controller may be thought of as a low-pass filter having attenuation characteristics governed by the strategy rules and execution rate. These characteristics were studied by cyclically perturbing the quantity TWR with a triangular wave, D(t), and noting the effect on V(t). Figure II-6 is a plot of the results of such a test. As shown in the figure, the period D(t) is 1.05 seconds which is equivalent to exactly 10.5 strategy moves (1 move = 100 msec). The results are summarized below.

| | Frequency of Perturbation | Calculated Max. Response in V(t) | Actual Average Response in V(t) |
|---|---|---|---|
| Trial-and-Error Strategy | 0.953 cps | 50 RPM | 22.5 RPM |
| MSA Strategy | 0.953 cps | 50 RPM | 40.0 RPM |

It is seen that the MSA strategy was more responsive to the given perturbation. Thus, it has a higher cut-off frequency and is capable of handling more rapid process variations than the trial-and-error strategy.

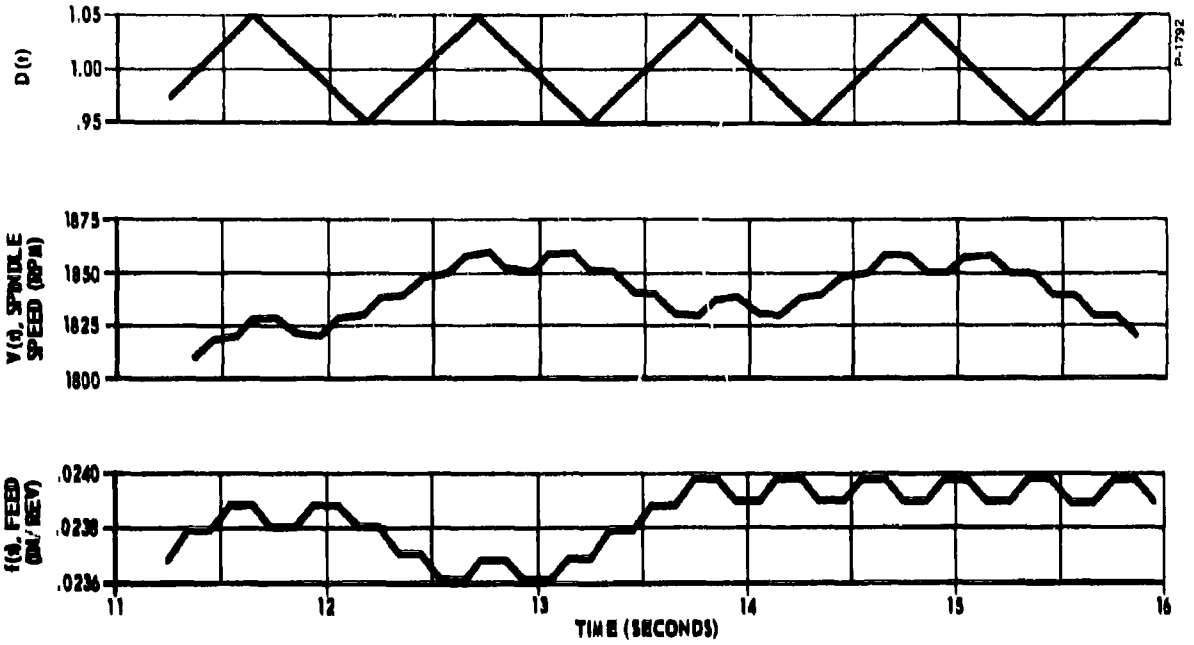


Figure II-6 - Effects of Small-Signal Perturbation on Speed and Feed

## Stability of Closed Loop

Two potential sources of system instability are (1) the existence of dynamic lags in the process which are long compared to the strategy execution rate and cause conventional servo instability; (2) the mismatching of the strategy and constraint correction logics so that they are mutually self-defeating and cause oscillatory "loops" to occur. A review of metalcutting literature indicates that dynamic lags in the actual milling process are quite small and are not likely to cause instabilities of the first type. The second type did occur, however, as a result of the initial choice of rules for the constraint correction logic.

An example of the type of oscillatory loop which occurred is as follows:

(a) An f-maximum constraint violation resulted during an f-exploration due to a +f increment.

(b) Operation switched to the constraint correction subroutine which removed the violation by executing a -f increment.

(c) Strategy operation was removed with another +f increment, causing a second f-maximum constraint violation.

(d) The pattern repeats indefinitely.

In order to eliminate the possibility of such loops occurring, the logic was modified so that a step which resulted in a previous violation cannot be repeated upon exit from the correction subroutine.

## Effectiveness of Constraint Violation Logic

A number of runs were made using the modified constraint logic for the purpose of evaluating its performance under a variety of situations. Figure II-7 is an example of one such run. This illustrates an MSA run in which operation is shown to proceed up to the maximum horsepower boundary, at which point a constraint violation occurs. The system then alternates between the constraint subroutine and the strategy subroutine, proceeding along the horsepower boundary until the maximum feed constraint is reached. The optimum point for this case is thus determined by the intersection of the horsepower and feed constraints.

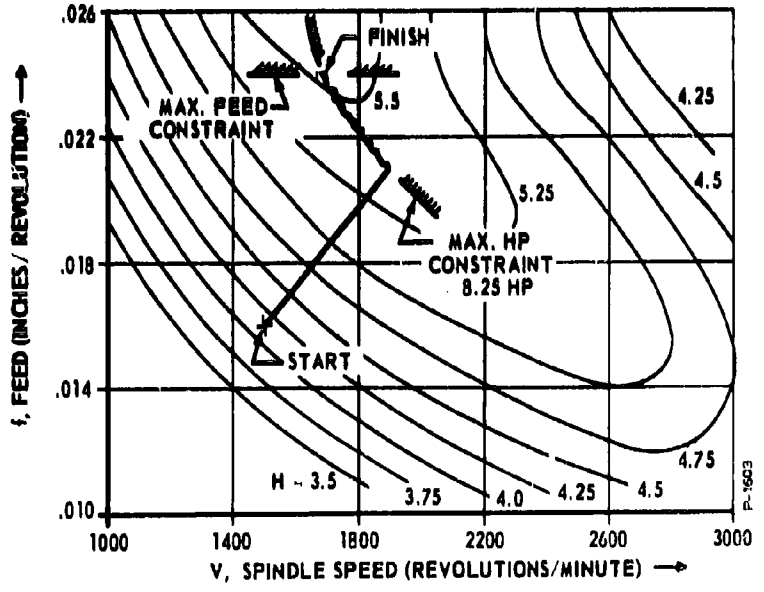


Figure II-7 - Plot of Steepest Ascent Run with Feed and Horsepower Constraints

The constraint logic functioned satisfactorily in all except two types of violation situations. In one of these, the optimum operating point was determined by the intersection of a maximum horsepower and a minimum spindle speed constraint, while in the other it was desired to travel along the horsepower constraint in the downward, rather than upward direction. Fortunately, neither of the above situations is expected to arise in practice, and they may be avoided entirely with proper choice of constraint limits and initial setpoints.

DISTRIBUTION LIST

| Addressee | Copy No. |
|---|---|
| Aeronautical Systems Division<br>Wright-Patterson Air Force Base, Ohio<br>Attention: ASRCT | 1 - 6 |
| Aeronautical Systems Division<br>Wright-Patterson Air Force Base, Ohio<br>Attention: ASRC (Mr. Ed Glass) | 7 |
| Aeronautical Systems Division<br>Wright-Patterson Air Force Base, Ohio<br>Attention: ASRCE (Mr. J. Teres) | 8 |
| Aeronautical Systems Division<br>Wright-Patterson Air Force Base, Ohio<br>Attention: ASRCEM-1A (Mrs. N. Ragen) | 9 & 10 |
| Northrop Aircraft Inc.<br>Dept. 5150-30<br>Hawthorne, California<br>Attention: A. Eskelin | 11 |
| Armed Services Technical Information Agency<br>ASTIA (TISIA-2)<br>Arlington Hall Station<br>Arlington 12, Virginia | 12 - 39 |
| The Foreign Technology Division<br>AFSC, TD-E2B<br>Wright-Patterson Air Force Base, Ohio | 40 |
| Cornell Aeronautical Laboratory, Inc.<br>Attention: Paul Rosenthal<br>P.O. Box 235<br>Buffalo 21, New York | 41 |
| Armour Research Foundation<br>Attention: Dr. S. Hori, Senior Engineer<br>10 West 35th Street<br>Chicago 16, Illinois | 42 |

| Addressee | Copy No. |
|---|---|
| Commander<br>U.S. N.O.T.S.<br>Pasadena Annex<br>Attention: J. H. Jannison<br>3202 E. Foothill Blvd.<br>Pasadena, California | 43 |
| Nortronics-Systems Support<br>Attention: Gordon Wilcox Lib<br>500 E. Orangethorpe Avenue<br>Anaheim, California | 44 |
| U.S. Atomic Energy Commission<br>Technical Information Service<br>P.O. Box 62<br>Oak Ridge, Tennessee | 45 |
| Aerojet General Corporation<br>Attention: Kenneth F. Mundt<br>V-P Manufacturing<br>6352 N. Irwindale Avenue<br>Azusa, California | 46 |
| Aerojet General Corporation<br>Attention: G. E. Jerhov<br>Fabrication Research<br>Numerical Control<br>Solid Rockets Plant<br>Sacramento, California | 47 |
| Aeronca Manufacturing Corporation<br>E. V. Gustanson<br>Director of Engineering<br>Middletown, Ohio | 48 |
| Aeronutronic<br>Division Ford Motor Company<br>Library<br>Ford Road<br>Newport Beach, California | 49 |

| Addressee | Copy No. |
|---|---|
| Aerospace Industries Association<br>Attention: B. S. Lee<br>610 Shoreham Bldg.<br>Washington 5, D. C. | 50 |
| Rohr Corporation<br>Attention: Nils O. Olesten, General<br>Supervisor, Numerical Control<br>P.O. Box 878<br>Chula Vista, California | 51 |
| Republic Aviation Corporation<br>Attention: A. Kastelowitz<br>Director Mfg. Research<br>Conklin Street<br>Farmingdale, L. I., New York | 52 |
| American Machine & Foundry Co.<br>Attention: Mr. Richard Dineen<br>Eng. Services Lab.<br>Box 889<br>Stamford,Connecticut | 53 |
| A. O. Smith Corporation<br>Attention: Fred Mackey<br>Box 584<br>Milwaukee, Wisconsin | 54 |
| Autonetics<br>Division of North American Aviation<br>9150 E. Imperial Highway<br>Downey, California | 55 |
| Avco Manufacturing Company<br>Lycoming Division<br>Attention: W. H. Panke, Supt. Mfg. Eng.<br>Stratford, Connecticut | 56 |
| Defense Metals Information Center<br>Battelle Memorial Institute<br>Attention: F. Boulger<br>505 King Avenue<br>Columbus 1, Ohio | 57 |

| Addressee | Copy No. |
|---|---|
| Bell Aircraft Corporation<br>Attention: R. W. Varrial<br>Mgr. Production Engrg.<br>P.O. Box 1<br>Buffalo, New York | 58 |
| (To Be Assigned) | 59 |
| General Electric Company<br>Attention: Mr. Joseph Bayer<br>Large Jet Engine Department<br>Mfg. Engrg. Research Laboratory<br>Cincinnati 15, Ohio | 60 |
| (To Be Assigned) | 61 |
| Boeing Airplane Company<br>Attention: L. Pickrell<br>Manufacturing Development<br>P.O. Box 3707<br>Seattle 24, Washington | 62 |
| Professor Orlan W. Boston<br>1645 Arbordale Drive<br>Ann Arbor, Michigan | 63 |
| The Norton Company<br>Attention: Dr. L. P. Tarasov<br>Research and Development Department<br>Worchester 6, Massachusetts | 64 |
| Chance-Vought Aircraft Company<br>Attention: E. G. Schuyler<br>P.O. Box 5907<br>Dallas, Texas | 65 |
| Cincinnati Milling Machine Company<br>Attention: Dr. M. Eugene Merchant<br>4701 Marburg Avenue<br>Cincinnati 9, Ohio | 66 |

| Addressee | Copy No. |
|---|---|
| Concord Control Inc.<br>Attention: Mr. J. O. McDonough, Pres.<br>1285 Soldiers Fld. Road<br>Boston 35, Massachusetts | 67 |
| General Dynamics/Astronautics<br>Attention: H. W. Holmerud<br>5001 Kearney Villa Road<br>San Diego 11, California | 68 |
| General Dynamics/San Diego<br>Attention: A. P. Langlois<br>Dept. 190-20<br>San Diego, California | 69 |
| General Dynamics/Fort Worth<br>Attention: Ralph A. Fuhrer<br>Chief Mfg. Engrg.<br>Ft. Worth, Texas | 70 |
| Curtiss-Wright Corporation<br>Wright Aeronautical Division<br>Attention: F. W. Mencik<br>Vice Pres. for Mfg.<br>Wood-Ridge, New Jersey | 71 |
| Douglas Aircraft Co., Inc.<br>Corporate Offices<br>Attention: Mr. W. J. Kinney, G-3<br>Numerical Control Coordinator<br>3000 Ocean Park Boulevard<br>Santa Monica, California | 72 |
| Douglas Aircraft Co., Inc.<br>Attention: N. H. Shappel, Works Mgr.<br>Santa Monica, California | 73 |
| Excello Corporation<br>Attention: Mr. Gordon A. Mcalpine<br>Ind. Sales Div.<br>P.O. Box 386<br>Detroit 32, Michigan | 74 |

| Addressee | Copy No. |
|---|---|
| Solar Aircraft Company<br>Attention: J. A. Logan<br>Mfg. Fac. Div.<br>San Diego 12, California | 75 |
| General Electric Company<br>Attention: Mr. D. O. Dice, Mgr. Mktg.<br>Waynesboro, Virginia | 76 |
| Giddings Lewis Machine Tool Company<br>Attention: Mr. K. S. Jensen<br>Fond du Lac, Wisconsin | 77 |
| Martin-Marietta Company<br>Attention: R. A. Bennett<br>P.O. Box 179<br>Denver 1, Colorado | 78 |
| Martin-Marietta Company<br>Attention: G. Bender, Sr. Mfg. Eng.<br>Mail 666<br>Baltimore 3, Maryland | 79 |
| Goodyear Aircraft Corporation<br>Attention: R. C. Abbott<br>Equipment Engineer<br>1210 Massillon Road<br>Akron 15, Ohio | 80 |
| Goodman Mfg. Company<br>Attention: Mr. Ken Stalker<br>48th Place & Halsted St.<br>Chicago, Illinois | 81 |
| Grumman Aircraft Eng. Corp.<br>Attention: William J. Hoffman<br>V-P of Mfg.<br>Bethpage, L. I., New York | 82 |
| Hiller Helicopter<br>Attention: Mrs. Marcia Nachtwly<br>Lib. Adv. Research Div.<br>Palo Alto, California | 83 |

| Addressee | Copy No. |
|---|---|
| Hughes Aircraft Company<br>Attention: D. F. Davern<br>Chief Tool Eng.<br>Tucson, Arizona | 84 |
| Hughes Tool Company<br>Attention: William W. Lampkin<br>Florence Ave. & Teale St.<br>Culver City, California | 85 |
| IBM Corporation<br>Manager, Laboratory Contracts<br>Department A07<br>Data Systems Division<br>P.O. Box 390<br>Poughkeepsie, New York | 86 |
| Jones and Lamson Machine Company<br>Manager of Research<br>Springfield, Vermont | 87 |
| Kaiser Aircraft Electric Corporation<br>Attention: Lloyd H. Walden<br>P.O. Box 275 Station A<br>Palo Alto, California | 88 |
| Kearney & Trecker Corporation<br>Attention: W. E. Brainard, Chief Eng.<br>Aircraft Tools<br>6784 W. National Ave.<br>Milwaukee, Wisconsin | 89 |
| Lockheed Aircraft Corporation<br>Attention: Robert L. Vaughn<br>Producibility Unit<br>2555 N. Hollywood Way<br>Burbank, California | 90 |
| Ladish Company<br>Attention: Mr. Paul Verdow<br>Asst. to Pres.<br>Cudahy, Wisconsin | 91 |

| Addressee | Copy No. |
|---|---|
| Lockheed Aircraft Corporation<br>Attention: K. H. Coleman<br>Coordinator Numerical Control<br>Dept. 11-01, Bldg. 72<br>Burbank, California | 92 |
| Lockheed Aircraft Corporation<br>Attention: H. Fletcher Brown<br>Manufacturing Mgr.<br>Marietta, Georgia | 93 |
| Lycoming Div. Avco Mfg. Corporation<br>Attention: Mr. Wayne Stone Sor.<br>Mfg. Eng. Anal. & Liaison<br>Div. Engineering Standards<br>Stratford, Connecticut | 94 |
| Marquardt Aircraft Corporation<br>Attention: Director of Mfg.<br>16555 Saticoy St.<br>Van Nuys, California | 95 |
| Martin-Marietta Company<br>Attention: Lloyd W. Kistler<br>Mfg. Engineer<br>Denver 1, Colorado | 96 |
| McDonnell Aircraft Corporation<br>Attention: Mr. Arthur J. Burke, Chief<br>Methods Eng.<br>Lambert-St. Louis Mun Airport<br>Box 516<br>St. Louis 66, Missouri | 97 |
| Ryan Aeronautical Company<br>Attention: Robert L. Clark<br>Vice-Pres. Mfg.<br>2701 Harbor Drive<br>San Diego 12, California | 98 |

| Addressee | Copy No. |
|---|---|
| North American Aviation, Inc.<br>Attention: Mr. Lou E. Frost, D/077<br>International Airport<br>Los Angeles 9, California | 99 |
| North American Aviation, Inc.<br>Attention: Mr. D. H. Ross, Dept. 64<br>4300 E. Fifth Avenue<br>Columbus, Ohio | 100 |
| Thompson Ramo Wooldridge, Inc.<br>Attention: D. P. Bloss<br>Dage Division<br>455 Sheridan Avenue<br>Michigan City, Indiana | 101 |
| Metcut Research Associates, Inc.<br>Attention: John F. Kahles<br>3980 Rosslyn Drive<br>Cincinnati 9, Ohio | 102 |
| (To Be Assigned) | 103 - 107 |
| The Library<br>United Aircraft Corporation<br>400 Main Street<br>East Hartford 8, Connecticut | 108 |
| (To Be Assigned) | 109 - 125 |
| Ray Data Corporation<br>Attention: Mr. Hall Cary<br>1078 East Granville Road<br>Columbus 24, Ohio | 126 |
| Carnegie Institute of Technology<br>Attention: Dr. M. C. Shaw<br>Pittsburgh, Pennsylvania | 127 |
| Micrometrical Manufacturing Company<br>3621 South State Street<br>Ann Arbor, Michigan<br>Attention: D. H. Parkes | 128 |

| Addressee | Copy No. |
|---|---|
| The Sheffield Corporation<br>721 Springfield Stree<br>Dayton 1, Ohio<br>Attention: Norman Jeglum | 129 |
| Aerospace Industries Association of America<br>Attention: Mr. S. A. Daniels, Dir.<br>Technical Services<br>1725 DeSales Street, N.W.<br>Washington 6, D. C. | 130 |
| Marquette University<br>Attention: Prof. A. O. Schmidt,<br>Mechanical Engineering<br>1515 W. Wisconsin Avenue<br>Milwaukee 3, Wisconsin | 131 |
| Pratt & Whitney Company, Inc.<br>Attention: E. E. Kirkham, Manager<br>Advance Engineering Section<br>Charter Oak Boulevard<br>West Hartford 1, Connecticut | 132 |
| Lear Siegler, Inc.<br>Astro Structures Division<br>Attention: B. P. Sernka<br>1700 E. Grand Avenue<br>El Segundo, California | 133 |
| Arthur D. Little, Inc.<br>Attention: David N. Smith<br>Acorn Park<br>Cambridge 40, Massachusetts | 134 |
| Mr. William B. Johnson<br>Numerical Control Coordinator<br>Dept. 564-02<br>Rocketdyne Division<br>North American Aviation, Inc.<br>Canoga Park, California | 135 |

| Addressee | Copy No. |
|---|---|
| Mr. P. K. Murphy<br>Superintendent Mfg. Services<br>Rocketdyne Division<br>North American Aviation, Inc.<br>Canoga Park, California | 136 |
| National Machine Tool Builders Association<br>Attention: Mrs. M. Bartlett<br>2139 Wisconsin Avenue<br>Washington 7, D. C. | 137 |
| Pratt & Whitney Company, Inc.<br>Attention: W. R. Skelley, Research Administrator<br>Charter Oak Boulevard<br>West Hartford 1, Connecticut | 138 |
| Motion Indicating Devices<br>Attention: Earl H. Kasselau<br>P.O. Box 158<br>Buffalo 23, New York | 139 |
| Baldwin Electronics, Inc.<br>Attention: C. Farrell Winder<br>6686 Hitching Post Lane<br>Cincinnati 30, Ohio | 140 |
| Technical Marketing Associates, Inc.<br>Attention: Courtland S. Randall, Vice-President<br>33 Sudbury Road<br>Concord, Massachusetts | 141 |
| Applied Machine Research<br>Attention: A. R. Campbell<br>1000 Macy Street<br>Los Angeles 33, California | 142 |
| (To Be Assigned) | 143 |
| Sandia Corporation<br>Attention: E. P. Quigley<br>Sandia Base<br>Albuquerque, New Mexico | 144 |

| Addressee | Copy No. |
|---|---|
| Major R. Kevin Murray<br>423 Woodring Way<br>Mather AFB, California | 145 |
| Mr. H. T. Johnson, Manager<br>Numerical Control Equipment Development Dept.<br>Ford Motor Company<br>Research & Engineering Center<br>Room 211-E, Dynamometer Building<br>Dearborn, Michigan | 146 |
| (To Be Assigned) | 147 - 149 |
| Aeronautical Systems Division<br>Wright-Patterson Air Force Base, Ohio<br>Attention: ASAPT | 150 |

Additional experimental work is required to correlate surface microfinish with sensed variables.

IV. Centner, R. M.
V. Avl for OTS
VI. In ASTIA collection

Research and Technology Division
Wright-Patterson Air Force Base, Ohio.
DEVELOPMENT OF ADAPTIVE CONTROL TECHNIQUES FOR NUMERICALLY-CONTROLLED MILLING MACHINES. Interim Technical Documentary Progress Rpt. Nr IR II 1 January 1963 - 31 July 1963. 84 p. incl. illus., tables. 6 refs.

Unclassified Rpt.

The detailed design of a complete adaptive control system is described. The results of an experimental metalcutting program indicate that instantaneous tool wear rate correlates with certain of the sensed variables. An empirical equation for calculation of this parameter was developed.

( over )

1. Machine-Milling
2. Machine Control-Numerical
3. Machine Control-Adaptive
4. Adaptive Control-Milling Machines
5. Machining Process Performance Optimization

I. RTD Proj. 7-713
II. Contract AF 33(657)-8782
III. Bendix Research Laboratories Division

Additional experimental work is required to correlate surface microfinish with sensed variables.

IV. Centner, R. M.
V. Avl for OTS
VI. In ASTIA collection

Research and Technology Division
Wright-Patterson Air Force Base, Ohio.
DEVELOPMENT OF ADAPTIVE CONTROL TECHNIQUES FOR NUMERICALLY-CONTROLLED MILLING MACHINES. Interim Technical Documentary Progress Rpt. Nr IR II 1 January 1963 - 31 July 1963. 84 p. incl. illus., tables. 6 refs.

Unclassified Rpt.

The detailed design of a complete adaptive control system is described. The results of an experimental metalcutting program indicate that instantaneous tool wear rate correlates with certain of the sensed variables. An empirical equation for calculation of this parameter was developed.

( over )

1. Machine-Milling
2. Machine Control-Numerical
3. Machine Control-Adaptive
4. Adaptive Control-Milling Machines
5. Machining Process Performance Optimization

I. RTD Proj. 7-713
II. Contract AF 33(657)-8782
III. Bendix Research Laboratories Division